INSTITUTO POLITÉCNICO DE BRAGANÇA
Escola Superior de Tecnologia e Gestão

Profitability study of the recovery of the expansion energy at the CPR natural gas station

Asma Cherbib

Dissertation presented to the School of Technology and Management of Polytechnic Institute of Bragança to the Fulfillment of the Requirements for the Master of Science Degree in Renewable Energy and Energetic Efficiency

Supervisor:

Prof. Paulo Miguel Pereira de Brito

Bragança

June, 2024

Acknowledgments

I would like to express my deepest gratitude to my beloved family for their unwavering love, encouragement, and support throughout this journey. Their endless sacrifices, understanding, and belief in me have been my source of strength and motivation.

To my friends, thank you for standing by my side, offering your support, and cheering me on during both the highs and lows of this academic endeavor. Your camaraderie and laughter have made this journey more enjoyable and memorable.

I am profoundly grateful to my supervisor, Mr. Paulo Miguel Pereira de Brito, for his invaluable guidance, expertise, and unwavering commitment to my academic and personal growth. His mentorship, encouragement, and constructive feedback have been instrumental in shaping this thesis and expanding my horizons.

I am also grateful to Mr. Amidi Jalloul, the Director of the Central Rades, for providing the essential information that contributed to the completion of this thesis.

I extend my heartfelt appreciation to the Polytechnic Institute of Bragança for providing me with the opportunity to pursue my master's degree in Renewable Energy and Energy Efficiency. The rich academic environment, resources, and support from faculty and staff have been indispensable in shaping my academic journey.

Finally, I would like to thank my esteemed professors, colleagues, and all those who have contributed in any way to my academic and personal development. Your collective efforts have left an indelible mark on my journey, and I am deeply grateful for your guidance, encouragement, and inspiration.

Abstract

This study embarks on a detailed examination of cutting-edge technological innovations grounded in physicochemical analysis, focusing on the thermodynamic behavior of natural gas within the Gas Expansion Station (GES). Our primary objective is to rigorously evaluate the feasibility and economic viability of recovering latent energy dissipated during the pressure reduction process at the GES, specifically within the operational context of the Rades Production Center Step-B.

Through comprehensive and systematic analysis, our research uncovers substantial potential in energy recovery initiatives. Key findings include the potential for an annual electricity production of 9.33 gigawatt-hours (GWh), resulting in significant financial savings exceeding 1,146,312 euros for consumers. Additionally, this approach is poised to drastically reduce greenhouse gas emissions, thereby contributing to environmental sustainability.

These findings are deeply interwoven with the complex production dynamics across various segments of the CPR. Therefore, our study not only explores the economic feasibility but also emphasizes the critical importance of sustainability and environmental responsibility within the energy sector.

In summary, our research highlights the transformative potential of harnessing latent energy resources, paving the way towards a future characterized by sustainability, resilience, and economic prosperity.

Keywords: Thermodynamic cycle, Gas Expansion Station (GES), Sustainability, Economic viability.

Resumo

Este estudo inicia uma análise detalhada das inovações tecnológicas de ponta baseadas em análise físico-química, focando-se no comportamento termodinâmico do gás natural na Estação de Expansão de Gás (GES). O nosso principal objetivo é avaliar rigorosamente a viabilidade e a viabilidade económica de recuperar a energia latente dissipada durante o processo de redução de pressão na GES, especificamente no contexto operacional do Centro de Produção de Rades Etapa-B.

Através de uma análise abrangente e sistemática, a nossa pesquisa revela um potencial substancial em iniciativas de recuperação de energia. As principais descobertas incluem a possibilidade de uma produção anual de eletricidade de 9,33 gigawatts-hora (GWh), resultando em economias financeiras significativas superiores a 1.146.312 euros para os consumidores. Além disso, esta abordagem está preparada para reduzir drasticamente as emissões de gases de efeito estufa, contribuindo assim para a sustentabilidade ambiental.

Estes resultados estão profundamente interligados com a dinâmica complexa da produção em vários segmentos do CPR. Portanto, o nosso estudo não só explora a viabilidade económica, mas também enfatiza a importância crítica da sustentabilidade e da responsabilidade ambiental no setor energético.

Em resumo, a nossa pesquisa destaca o potencial transformador de aproveitar os recursos energéticos latentes, abrindo caminho para um futuro caracterizado por sustentabilidade, resiliência e prosperidade económica.

Palavras-chave: Ciclo termodinâmico, Estação de Expansão de Gás (GES), Sustentabilidade, Viabilidade económica.

Table of Contents

Table of Contents iv

List of Figures vii

List of Tables viii

Acronyms ix

1. Introduction 1

1.1 Background 1

1.2 Objectives 2

1.3 Document structure 2

2. Context of the study 3

2.1 Presentation of the company 3

2.2 General description and operation of a production unit of the Rades production center. 3

2.2.1 Equipment existing at Rades Production Center A and B 4

2.2.2 Natural gas system of the power plant 5

2.3 General information on pipelines 6

2.3.1 Gas pipelines 6

2.4 Fuel supply plant 7

2.4.1 Natural gas overview in Tunisia 7

2.4.2 Fuel gas supply system 8

2.5 Problem statement 11

2.6 Current solution and technologies 12

3. Thermal resources in industry 14

3.1 Introduction 14

3.2 Heat recovery in industry 14

3.2.1 General information on waste heat recovery in industry 14

3.2.2 The principles of heat recovery 15

3.2.3 Heat recovery options and technologies 15
3.3 General information on combustion 24
3.3.1 Advanced Combustion Analysis and Practical Calculations 25
3.4 Thermodynamic properties of reacting species 30
3.4.1 Internal Energy and Enthalpy : 30
3.4.2 Heat of Reaction: 30
3.4.3 Application in Combustion Analysis: 30
4. System modeling 32
4.1 Introduction 32
4.2 Natural gas pressure-reducing station 32
4.2.1 General system description and operation 32
4.2.2 Technical description of the supply 33
4.3 Simple recovery of expansion energy by a turbogenerator 36
4.3.1 Turbogenerator functionality 37
4.3.2 Energy balance of the system 38
4.3.3Natural gas expansion in the turbine 38
4.3.4 Condensate and hydrate formation 39
4.4 Sizing the Turbine 40
4.4.1 Turbine performance 41
4.4.2 Calculating power supplies 42
4.5 Preheater equipment selection 42
4.5.1 Thermal analysis 42
4.5.2 Choice of co-generator (gas engine) 44
4.5.3 Estimation of exhaust gas properties 45
4.6 Sizing the flue gas/water heat exchanger 50
4.6.1 Beam geometry 51
4.6.2 Calculating the dynamic viscosity and thermal conductivity of smoke 52

4.6.3 Wall temperature profile 53
4.6.4 Reference values 54
4.6.5 Calculation of the average exchange coefficient 55
4.7. Sizing the gas/water heat exchanger 60
4.7.1 Water mass flow calculation 60
4.7.2 Calculating the exchange surface between water and natural gas 60
4.7.3 Calculating heat exchanger dimensions 60
4.8 Hypotheses on exchanger analysis 61
4.9 Intermediate circuit pump sizing 62
4.10 Motor sizing 63
4.10.1 Functionality 63
4.10.2 Gas mixture composition 64
4.10.3 Consumed gas flow 66
4.10.4 Combustion power 67
4.11 Integrated Environmental and Financial Impact Assessment 67
4.11.1 Environmental impact assessment 67
4.11.2 Financial Statement 69
5. Conclusions 70
Reference 72
Appendices 75

List of Figures

Figure 1. Operating principle of a thermal unit. [3] 4
Figure 2. Positional relationships between gas fields and pipelines in Tunisia. [4] 8
Figure 3. Schematic diagram of natural gas pipeline. [4] 9
Figure 4. Diagram of the natural gas circuit of a thermal power plant. [2] 10
Figure 5. Heat rejection sources; Recovery technology and final use recovered heat. 14
Figure 6. Temperature distribution in a parallel co-current exchanger.[6] 19
Figure 7. Temperature distribution in a countercurrent exchanger.[6] 20
Figure 8. Latent heat losses [7] 29
Figure 9. PRS installation diagram [8] 33
Figure 10. Radial reaction turbine. [9] 37
Figure 11. Simple PRS block Diagram. 39
Figure 12. Gas evolution in the turbo-generator system. [10] 39
Figure 13. Moullier diagram for methane. [12] 41
Figure 14. Preheater feed by Steam Transformer. 43
Figure 15. Preheater supply from a boiler. 43
Figure 16. Preheater supply from a cogenerator. 44
Figure 17. Flow perpendicular to the tube bundle. 50
Figure 18. Staggered beam. 51
Figure 19. In-line beam. 51
Figure 20. Tubular cross-current exchanger Left: opposite inlets. Right: inlets on the same side. 53
Figure 21. Temperature profile during exchange through a surface element dS. [21] 53
Figure 22. Intermediate hydraulic circuit. [16] 62
Figure 23. Beau de Rochas cycle. [17] 63

List of Tables

Table 1.Description of Rades A and B thermal power plants. [4] 4
Table 2. Specification of main equipment for Rades A and B power plants. [4] 5
Table 3. The hourly natural gas consumption at the time of each plant's rated capacity. [4] 9
Table 4. Current Turbo Generator Technologies 12
Table 5. Air composition 25
Table 6. Existing heater characteristics. (see Appendix 4)..... 35
Table 7. The Dew-point temperature calculation. 40
Table 8. Natural gas characteristics for each stage in the system. 41
Table 9. Characteristic table of two fluids [13] 42
Table 10. Composition of the natural gas fed to the combustion chamber. (Appendix 7) .. 46
Table 11. Fume composition in mass and molar fractions 47
Table 12. Molar heat capacities at constant pressure Cp ($\boldsymbol{J}.\boldsymbol{mol}$-1 $\boldsymbol{K}$-1) for different temperatures. [13]..... 47
Table 13. Molar heat capacity at constant volume $\boldsymbol{Cv}$ ($\boldsymbol{J}.\boldsymbol{mol}$-1 $\boldsymbol{K}$-1) for different temperatures. [13]..... 48
Table 14. Composition of flue gases with excess air in mass and molar fractions 49
Table 15. Fume characteristics at Tm =305°C and atmospheric pressure..... 52
Table 16. Combustible and smoke-producing with and without excess air 65
Table 17. Density and mass flow of gases..... 66
Table 18. Natural Gas LHV 67

Acronyms

CCPP: Combined Cycle Power Plant

CHP: Combined heat and power

CPR: Rades Production Center

GDP: Gross Domestic Product

GHG: Greenhouse Gas

HHV: Higher Heating Value

LHV: Lower Heating Value

MHI: Mitsubishi Heavy Industry

NG: Natural Gas

NTU: Number of Transfer Units

PFD: Process Flow Diagram

PRS: Pressure Regulating Station

ST: Steam Transformer

STEG: Tunisian Company of Electricity and Gas

TPP: Thermal Power Plant

1. Introduction

In recent years, Tunisia has faced significant challenges stemming from both internal transitions and external economic pressures. Amidst a backdrop of democratic transitions and social upheavals, the country has grappled with economic instability exacerbated by volatile international markets. Of particular concern has been the sharp increase in hydrocarbon prices and the depreciation of the Tunisian dinar against foreign currencies. These factors have imposed a heavy burden on institutions like STEG (Tunisian Company of Electricity and Gas), leading to challenges in meeting financial obligations and sustaining operations.

At the heart of these challenges lies the fuel bill, which is closely tied to the international price of natural gas. The reluctance to settle bills post-Revolution has further strained the financial resources of energy providers like STEG, resulting in a significant backlog of receivables. As of the latest reports, receivables account for approximately 15.7% of the total billed amounts. This indicates a substantial portion of billed revenues remains uncollected, underscoring the urgent need for financial stability and the development of sustainable revenue streams.

Despite these challenges, the global energy landscape presents additional concerns, including the potential shortage of fossil fuels such as natural gas. While renewable energies offer promise, they cannot yet fully meet the energy demands of all sectors, leaving a critical gap in energy supply. In response, austerity measures and effective resource management are imperative, particularly in the management of hydrocarbons.

1.1 Background

In the face of these challenges, STEG has demonstrated resilience and adaptability, actively pursuing solutions to enhance energy efficiency and explore alternative energy sources. Projects such as biogas valorization, harmonics disturbance control, and energy recovery from gas stations exemplify the organization's commitment to innovation and sustainability. By harnessing emerging technologies and leveraging available resources, STEG has sought to diversify its energy portfolio and reduce reliance on conventional fuels.

However, the focus has now shifted towards the untapped potential of waste heat recovery. Recognizing the significant energy losses associated with industrial processes, STEG aims to optimize energy usage by capturing and utilizing waste heat effectively. By investing in

heat recovery technologies and implementing efficient systems, the organization seeks to minimize environmental impact, reduce operating costs, and enhance overall energy resilience.

1.2 Objectives

This project aims to implement advanced technology to recover energy lost during gas expansion at the Rades thermal power plant. This process involves conducting comprehensive physicochemical analyses of the thermodynamic cycle of natural gas to accurately design and deploy an efficient heat recovery system. Combining theoretical studies, technical evaluations, and practical implementation, the goal is to optimize energy recovery while minimizing environmental impact. Ultimately, this project seeks to provide actionable insights and recommendations for sustainable energy production in Tunisia, contributing to regional development and energy sustainability initiatives.

1.3 Document structure

This Dissertation report is organized into five chapters. In the first chapter, a brief introduction to the study is carried out and its objectives are presented. The second chapter will address the problem of energy production in general and in particular in the gas and electricity production sector. A third chapter will introduce waste heat in industry as well as an overview of recovery techniques and exploitation tools. It will also define some chemical and thermodynamic relations necessary for the further work. The fourth chapter is a technical study in which we will use all that is already announced in the previous chapters in order to obtain the objective results of our study. The last chapter is the presentation of the main general conclusions and the proposal of a few possibilities for future projects.

2. Context of the study

2.1 Presentation of the company

he Tunisian Company of Electricity and Gas (STEG) is a public law company with a non-administrative character. Established in 1962, its mission is the production and distribution of electricity and natural gas throughout Tunisia. STEG is the second-largest Tunisian company by turnover. Its main objective is to serve the national market with electricity and gas to meet the country's development needs. Electricity accounts for about 6% of the Gross Domestic Product (GDP), and the average individual electricity consumption of Tunisians is approximately 1,550 kWh per year, the highest among countries in the southern Mediterranean basin, despite Tunisia's relatively limited energy resources. **[1]**

2.2 General description and operation of a production unit of the Rades production center.

The Rades Power Plant (C.P Rades) plays a crucial role in generating electrical energy by harnessing the chemical energy released through combustion in a steam generator, or boiler. This process transforms water into dry steam and superheats it to reach 540°*C* and 138 bars of pressure. This represents the conversion of chemical energy into heat energy (Figure 1). The superheated steam drives the high-pressure (HP) turbine rotor into rotation and undergoes expansion at the exit of the HP turbine stage. Subsequently, it returns to the boiler for reheating to 540°C before being redirected to the intermediate-pressure (IP) and low-pressure (LP) turbine stages for further expansion.

The reheating of steam serves to increase the thermal efficiency of the unit and prevent any thermal stresses on the turbine shaft. During these successive expansions, heat energy is converted into mechanical energy available on the turbine shaft. This mechanical energy is then transmitted to the alternator, which functions as an alternating current generator, to produce electrical energy with a voltage of 15.5 kV.

The exhaust steam from the turbine (LP stage) enters the condenser to be condensed through the conduction phenomenon, facilitated by the presence of a cold source, seawater, which is pumped into the condenser via circulation pumps. After condensation, the water is conveyed by extraction pumps to the LP heater to be gradually reheated before being returned to the

boiler through feedwater pumps. This progressive reheating of water aims to increase the efficiency of the boiler and prevent thermal stresses on its walls. This water station consists of a number of heat exchangers supplied with steam by extraction from the three turbine stages. Finally, the cycle repeats indefinitely since steam and water circulate in a closed circuit. **[2]**

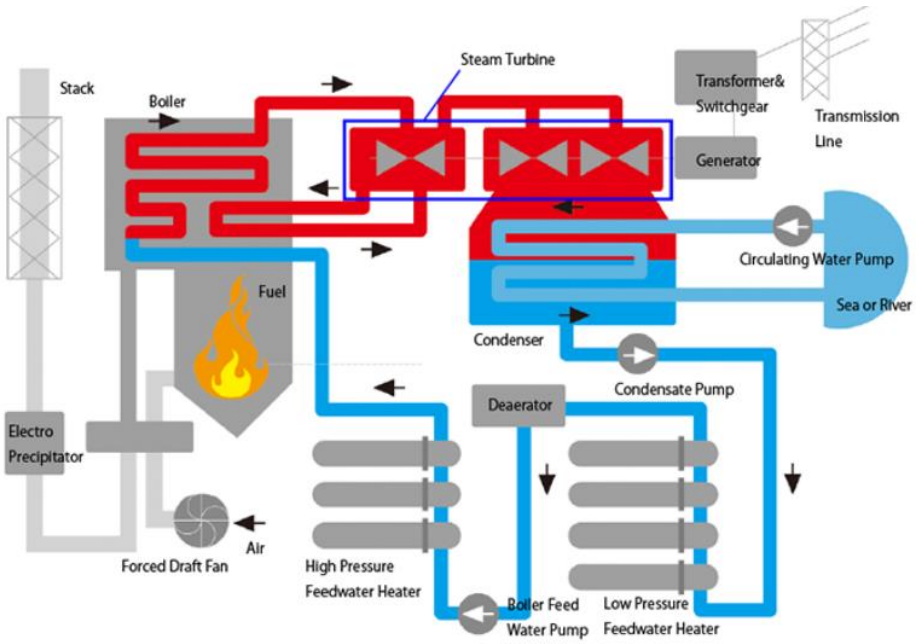

Figure 1. Operating principle of a thermal unit. [3]

2.2.1 Equipment existing at Rades Production Center A and B

The Rades Power Plant consists mainly of four steam generators and four turbo generator sets. A description of Rades A and B, including their year of construction, is presented in Table 1.

Table 1.Description of Rades A and B thermal power plants. [4]

	Rades A	Rades B
Year of construction	1985	1998
Installed power	340 MW	360 MW
Manufacturer	MHI	Ansaldo
Electricity production	12 % of electricity production by STEG	

Rades A was put into operation in 1985 and has an installed capacity of 340 MW (2 units of 170 MW), while unit B was put into operation in 1998 and has an installed capacity of 360 MW (2 units of 180 MW).

Specifications of the main equipment of the plant are presented in Table 2. The main equipment, such as the boiler, steam turbine and generator, were built and supplied by the Japanese companies Mitsubishi Heavy Industries (MHI) and Ansaldo.

Table 2. Specification of main equipment for Rades A and B power plants. [4]

		Rades A		Rades B	
		Unit 1	**Unit 2**	**Unit 1**	**Unit 2**
1	**Steam Turbine**				
	Manufacturer	Mitsubishi Heavy Industries (MHI)		Ansaldo	
	Capacity	170 MW each		180 MW each	
	Type	Tandem compound, single envelope, condensation double flow		HD1R-MD1-ND31 AU	
	Setting into service	1984		1997	
2	**Generator**				
	Manufacturer	Mitsubishi Electric Corporation (MELCO)		Ansaldo	
	Type	MB-J		THR-2-232000	
	Setting into service	1984		1996	
3	**Boiler**				
	Manufacturer	MHI		Ansaldo	
	Capacity	530 t/h each		536 t/h each	
	Number of burners	28 each		12 each	

2.2.2 Natural gas system of the power plant

Natural gas is one of the most widely used fuels in thermal power plants because it is easier to handle and cleaner than coal or heavy fuel oil. The operation of natural gas requires special structure, equipment, instruments and automatic control. The use of natural gas in thermal power plants has many special features compared to other fuels:

- Absence of solid waste, thus the absence of fouling and erosion of steam generator exchanger bundles.

- Absence of sulphureous hydride formation, therefore absence of corrosion of the low temperature parts of the combustion gas circuit.
- Very flexible combustion, easily adaptable to automatic controls.
- Possibility of combustion with a very low excess of air with a more elaborate regulation.
- Reduction of maintenance costs.
- Improved efficiency of steam generators.

The C.P Rades is supplied with natural gas from the national distribution grid of 16-20 bars. The gas undergoes several preparation operations before being introduced into the boiler, it must be filtered, heated, expanded and counted.

2.3 General information on pipelines

A pipeline is an underground or above-ground conduit used for transporting goods, whether in liquid or gaseous form. Pipelines are typically constructed from welded steel tubes, externally or internally coated, and generally buried in the ground. These pipelines can be costly and sometimes challenging to implement depending on the characteristics of the terrain, especially in seismic or unstable areas. Despite their initial investment, their ongoing usage tends to be relatively inexpensive compared to other competing forms of transportation, at least for short to medium distances.**[5]**

The type and name of a pipeline depend on the physical characteristics and transportation conditions of the product being conveyed:

- For natural gas, we use the term gas pipeline.
- For oil, we use the term oil pipeline.
- For oxygen, the term oxygen pipeline or oxyduct is used.

In general, the Latin suffix "ductus," derived from "ducere," meaning "to lead" or "to conduct," is used to define the French name of a specialized pipeline for the transportation of a specific type of product.

2.3.1 Gas pipelines

The majority of gas pipelines transport natural gas between extraction zones and consumption or export zones. The total length of gas pipelines worldwide is estimated at one million kilometers, or more than 25 times the earth's circumference. Most gas pipelines are laid on land, either buried at a depth of around one meter in populated areas, or laid directly on the ground in desert or hard-soil zones. Their diameter varies from 50 mm (2 inches) to

1400 mm (56 inches) for the largest. However, the drying up of local sources and the increasing remoteness of exploitation areas have led to the establishment of submarine pipelines. Depending on their nature of use, pipelines can be classified into three main families.**[5]**

- Gathering pipelines: bringing the gas from the fields or underground storage to the processing sites.
- Transmission or transit pipelines: transporting processed gas (dehydrated, desulfurized, etc.) at high pressure to urban areas or industrial consumption sites.
- Distribution pipelines: distributing gas at low pressure as close as possible to domestic consumers or small industries.

2.4 Fuel supply plant

2.4.1 Natural gas overview in Tunisia

Tunisia is an oil and natural gas-producing country. According to statistics from the U.S. Energy Information Agency, natural gas reserves in Tunisia were estimated at 2.3 trillion cubic feet (Tcf) in 2012. This figure is lower than that of neighboring countries, since Algeria has natural gas reserves amounting to 159 Tcf and Libya's reserves being 53 Tcf. Tunisia has a large number of gas fields, including the Miskar field which is endowed with the largest production volume, followed by the Hasdrubal field.

These two deposits are located offshore, east of Tunisia. In addition, a gas pipeline, called Trans-Mediterranean Gas Pipeline, crosses Tunisia and connects Algeria to Italy. This pipeline was built to supply Italy with natural gas from Algeria.

Starting from Hassi R'Mel in Algeria, the pipeline crosses Tunisia over a distance of about 370 km and reaches Italy via Sicily. It provides Italy with 5.25% of the total natural gas flowing through this pipeline without royalty charges. In addition, natural gas is imported from Algeria through this pipeline to meet Tunisia's natural gas demand. Figure 2 illustrates the positional relationships between gas fields and pipelines in Tunisia.

Figure 2. Positional relationships between gas fields and pipelines in Tunisia. [4]

2.4.2 Fuel gas supply system

The gas pipeline used to supply natural gas to the two TPP Rades A and B stages and La Goulette is a 16-inch (40.64 cm) diameter conduit, separately connected to the existing gas refueling station. It branches off within the station located at the Rades A and B site. Figure 3 illustrates the schematic diagram of the natural gas pipeline.

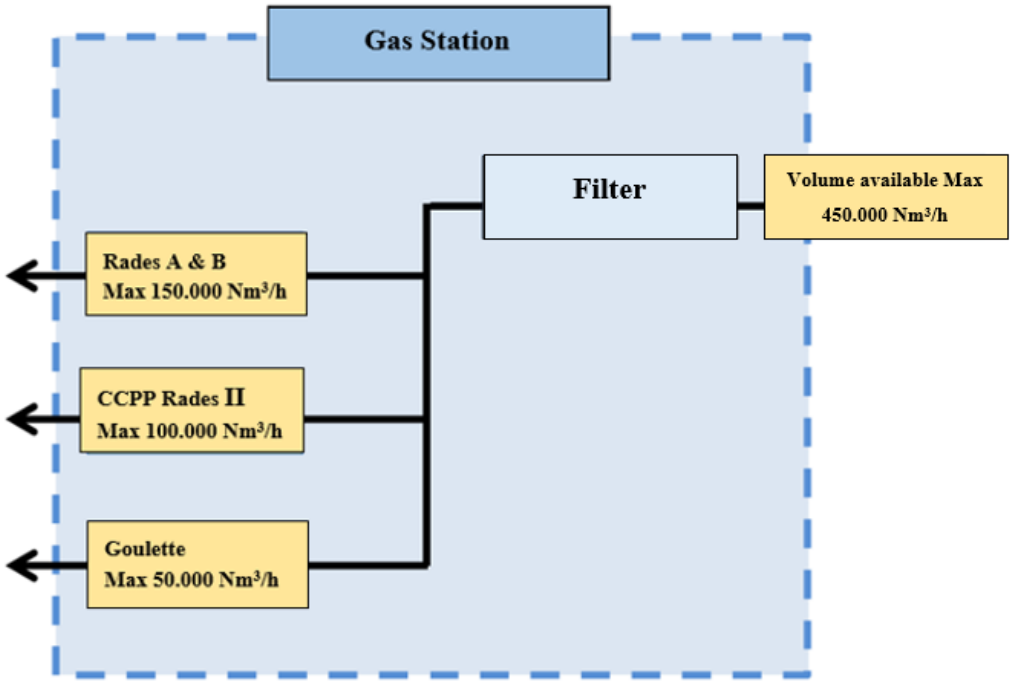

Figure 3. Schematic diagram of natural gas pipeline. [4]

Table 3. The hourly natural gas consumption at the time of each plant's rated capacity. [4]

Name of the station	Consumption in Gas Nm^3/h
Rades A & B	150 000
Rades II	100 000
Goulette Station	50 000
Total	300 000

Natural gas can be supplied up to the volume of 450,000 $Nm3/h$. In return, the total natural gas consumption of each power plant is 300,000 $Nm3/h$. Therefore, this shows that natural gas will be able to be supplied sufficiently to the Rades B power plant (The unit on which the profitability of the recovery of energy lost at the gas expansion station was studied).

The pressure of the natural gas feeding the burners and the igniters varies according to the requested combustion rate from 1.5 to 2.2 bars, the gas arrives at the C.P Rades at a pressure between 15 and 20 bars. It is therefore necessary to expand it so as to have a pressure close to 4 bars before the regulating valve. A second separate expansion for each steam generator regulating the pressure of about 2 bars upstream of the natural gas flow regulating valve.

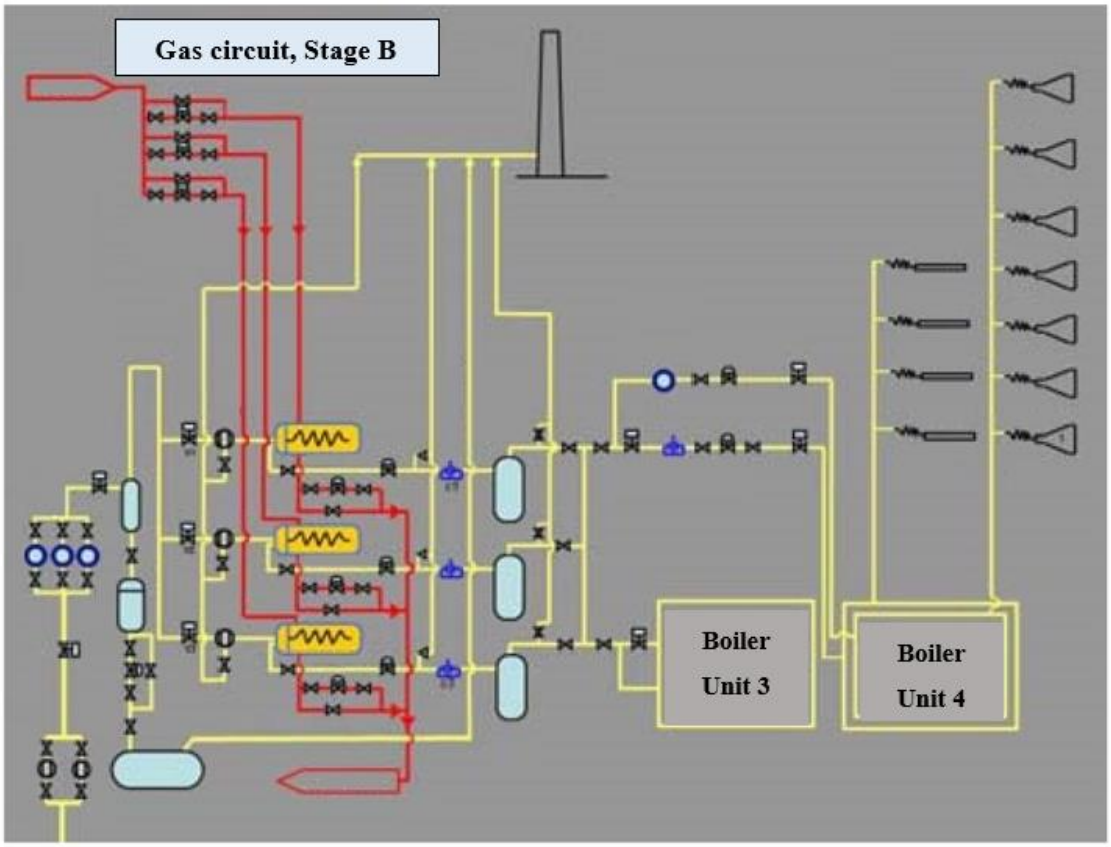

Figure 4. Diagram of the natural gas circuit of a thermal power plant. [2]

Depending on the type of regulator and the design of the regulator stations, the gas expansion can cause noises which are transmitted and sometimes amplified by the pipes, and can reach levels which are unacceptable for humans and for the good condition of the equipment. In critical cases, the importance of this phenomenon is reduced by muffling the noise in silencers placed immediately after the regulators. Any expansion of natural gas causes a temperature drop of 0.4°C/bars due to the Thomson Joule effect, which depends on the pressure drop in the regulator and the required gas flow. A drop in temperature can cause:

- The formation of methane hydrate crystals, which can completely block the pipes if the gas is not perfectly dry.
- External icing of regulators and valves, which can interfere with their operation.
- Disruption of the operation of diaphragm meters (temperature correction).

It is therefore necessary to heat the gas before its expansion in order to avoid its disadvantages by the use of conventional water or steam heaters fed by the water stations or the steam generators of the power plant when it is a question of heating the gas feeding a recovery turbine. The reheating is carried out before expansion by means of reheaters. A

regulation of the heat flow arrival (heating fluid) is necessary to maintain a temperature between 25 and 30°C after expansion.

A separator, placed at the head of the station, ensures a first elimination of the impurities which can be conveyed by the natural gas, generally the separator is menu of a settling pot. Filters ensure the final operation. These filters have an important role at the beginning of the operation. The dust and iron oxide contained in the gas lines are progressively carried to the primary expansion station. However, in installations where the gas circulates at high speed, these filters remain indispensable because of the continuous entrainment of oxides which could damage the regulators and burners.

A manometric device is installed in order to control the clogging. Some devices can, by their design, act as both separator and filter. Safety valves are used in multiple line installations, they are placed upstream of each regulator, they are used to isolate the expansion line in case of a fault. The safety valve is controlled by the gas pressure of the downstream circuit, so the closing of this valve depends only on the set pressure of the valve and must be done in consideration of the influence of the pressure loss and the possible drop of the regulator according to the gas flow.

The evacuation of an overpressure downstream of the pressure regulators is done by means of safety valves, which are mechanically controlled by the gas pressure in the downstream circuit where they are installed.

The fire-fighting stations must be sufficient in number and in perfect working order. In case of fire, the instructions must be perfectly known by all the personnel.

In case of maintenance work on the piping or the gas circuit equipment, this one will be completely purged, the tools used must be in bronze. The use of explosimeters is imperative in the vicinity of the expansion devices, to detect any presence of gas in the atmosphere and to indicate whether or not there is a risk of explosion **[2].**

2.5 Problem statement

The units of the gas station operate in parallel with pressure reduction valves on the gas network. It is through this pressure that the gas is conveyed in the pipelines of the gas distribution system. However, the pressure is too high to be used safely by the end user (thermal power plants). For gas to be suitable for industrial use, it must be available at less than 4 bars (this is the pressure of the gas used by a large gas boiler). At several points in the network, the gas passes through pressure reduction stations, where the gas pressure is

reduced by expansion through a valve. The pressure reduction performed in this way produces energy.

Any expansion of natural gas results in a decrease in temperature due to the Joule-Thomson effect, which depends on the pressure drop in the regulator and the gas flow rate demanded by using conventional water or steam heaters powered by a steam transformer. In most cases, this significant wasted energy, although it is possible to use it to produce mechanical work by using a reaction turbine instead of an expansion valve, and through a shaft connected to an alternator, it is therefore possible to produce electricity without emitting CO_2.

2.6 Current solution and technologies

Since the recovery of waste energy at the natural gas expansion station does not result in CO_2 emissions, the principle of the technique used is to transform the unused energy into electricity. The expansion of a fluid, such natural gas converts, kinetic energy into mechanical energy. By utilizing the expansion phenomenon, radial turbines are designed to capture the energy dissipated from the fluid (natural gas). This process results in the direct transformation (primary cycle) of kinetic energy into mechanical energy, which is then converted into electricity.

No gas is burned or consumed in this process, making it comparable to hydroelectric power, where the passage of water turns the turbine without altering the water quality. Three types of turbo-generators, designed to convert this expansion energy into electricity, are presented in Table 4 below **[5]**:

Table 4. Current Turbo Generator Technologies

Single-stage turbogenerator with oil bearings	**Multi-stage turbogenerator with oil bearings**	**Magnetic bearing turbine generator**
		
- Power output: from 500 kW to 15 MW	- Power output: from 500 kW to 15 MW	- Power output : to 300 kW
- Speed: from 6 000 rpm to 33 000 rpm	**- Speed: from 6 000 rpm to 33 000 rpm**	**- Speed : 30 000 rpm**

The objective of this project, is to install a turbogenerator at the PRS station of stage B located at Rades A and B, the purpose of which is to use the energy produced by lowering the pressure ($\approx 20\ bars$) of the gas pipeline to meet the local low-pressure distribution network to units 3 and 4. In other words, the 40,000 Nm^3/h gas flow is allowed to expand driving the turbine. The turbine wheel drives a gearbox coupled to a synchronous generator. The resulting power of electricity recovered in this way is then delivered to the STEG power grid.

3. Thermal resources in industry

3.1 Introduction

In this chapter, we will explore the concept of residual heat loss in industrial processes and discuss the various techniques available for heat recovery and utilization. We will provide a comprehensive overview of the tools and methods used to capture and exploit this lost energy. Additionally, we will delve into the necessary chemical and thermodynamic principles that underpin these processes, setting the foundation for the subsequent sections of our study. Our aim is to illustrate the potential of harnessing residual heat to improve energy efficiency and sustainability in industrial operations.

3.2 Heat recovery in industry

3.2.1 General information on waste heat recovery in industry

Efforts to improve energy efficiency focus on reducing the industrial energy consumed by equipment used in manufacturing (e.g., boilers, furnaces, dryers, reactors, separators, motors and pumps). A valuable alternative approach to improving overall energy efficiency is to capture and reuse the "waste heat" that is intrinsic to all industrial production. In some cases, such as industrial furnaces, efficiency improvements resulting from waste heat recovery can improve energy efficiency by 10% to nearly 50%. **[5]**

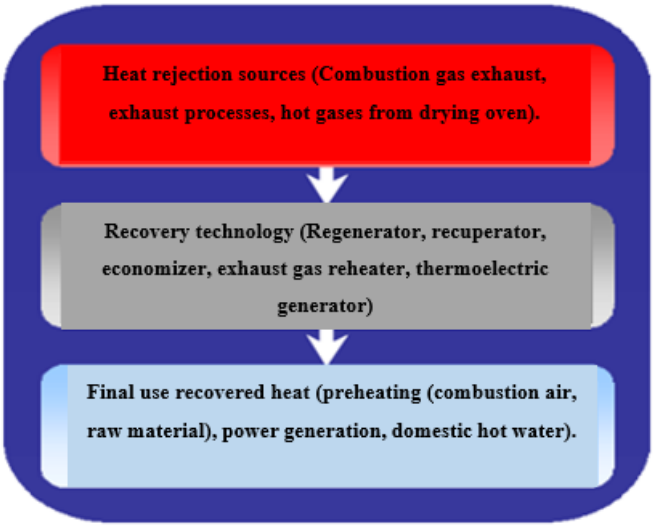

Figure 5. Heat rejection sources; Recovery technology and final use recovered heat.

Therefore, it is necessary to identify the research, development and demonstration technology needed to enable the continued recovery of heat loss from industrial waste. Three essential elements are needed for waste heat recovery:

- An accessible source of waste heat.
- A recovery technique.
- A use for the recovered energy.

3.2.2 The principles of heat recovery

Waste heat losses result from both equipment inefficiency and thermodynamic limitations on equipment and processes. Exhaust gases immediately leaving a gas engine can have temperatures as high as 400-500°*C*. Consequently, these gases have a high heat content, carrying as much as 60% of the energy input of the facility used. Efforts must be made toward more energy-efficient design with better heat transfer and lower exhaust temperatures, but the laws of thermodynamics impose a lower limit on the exhaust gas temperature. **[3]**

Since heat exchange involves transferring energy from a high-temperature source to a low-temperature sink, the temperature of the combustion gases must always be higher than the temperature required for the purpose of the installed equipment (such as the metal melting temperature for a smelting furnace or the driving pressure for an expansion turbine) to comply with the second law of thermodynamics. In this scenario, at least 40% of the energy input to the boiler is still lost as heat for aluminum smelting furnaces and more than 70% for gas engines. **[3]**

Recovery of industrial waste heat can be achieved through various methods. Heat can either be "reused" in the same process or transferred to another process. Ways to reuse heat locally include using combustion exhaust gases to preheat the feed fuel for industrial boilers, preheating feedwater before entering a heat exchanger (natural gas preheater). In this way, the recovered heat can replace fossil energy that would otherwise have been used in the facility. **[3]**

3.2.3 Heat recovery options and technologies

Heat recovery is essential for improving energy efficiency, reducing fossil fuel consumption, operating costs, and pollutant emissions. Various methods and technologies are employed based on the temperature ranges of the waste heat sources, categorized as high, medium, and low-temperature sources. Additionally, cogeneration systems offer a comprehensive approach to utilizing waste heat.

- **High-Temperature Sources (>650°C)**

High-temperature waste heat sources, such as smelting furnaces and kilns, involve processes where exhaust gases reach temperatures above 650°C. Smelting furnaces, used in metal extraction and refining, and kilns, utilized in ceramics and cement production, operate at very high temperatures, resulting in significant heat loss.

Technologies for recovering high-temperature waste heat include:

- Regenerative Burners: These burners use a pair of chambers filled with a ceramic medium. One chamber captures and stores heat from the exhaust gases, which is then used to preheat the incoming combustion air. This cyclic process significantly improves thermal efficiency.

- Waste Heat Boilers: These boilers capture the high-temperature exhaust gases to generate steam or hot water, which can be used for power generation or as process steam in various industrial applications.

- **Medium-Temperature Sources (230°C < T < 650°C)**

Medium-temperature waste heat sources are common in processes such as engines and turbines, where exhaust gases range between 230°C and 650°C. Internal combustion engines and gas turbines used in various industrial applications fall into this category.

Technologies for recovering medium-temperature waste heat include:

-Recuperators: Heat exchangers that recover heat from exhaust gases to preheat incoming air. This process increases combustion efficiency by reducing the energy required to heat the air.

-Economizers: Used in steam boiler systems, economizers capture waste heat from flue gases to preheat the boiler feedwater, thus improving the boiler's overall efficiency by reducing the fuel needed to heat the water.

- **Low-Temperature Sources (<230°C)**

Low-temperature waste heat sources involve processes with heat emissions below 230°C, such as industrial dryers and cooling water systems. Dryers in food processing and pharmaceuticals, and cooling systems in various industries, discharge warm air and water that can be utilized.

Technologies for recovering low-temperature waste heat include:

Heat Pumps: Devices that transfer heat from a cooler space to a warmer space using mechanical work. In industrial applications, heat pumps can upgrade low-temperature waste heat to a higher temperature, making it useful for space heating or other processes.

Heat Exchangers: Used to transfer heat between fluids without mixing them. In low-temperature applications, heat exchangers capture waste heat from processes like drying and cooling and reuse it to preheat incoming air or water.

- **Cogeneration Systems**

Cogeneration, or combined heat and power (CHP), is the simultaneous production of electricity and useful heat in the same plant. This concept leverages the heat generated during electrical production to meet thermal demands, such as heating, domestic hot water, and industrial processes.

Examples of cogeneration systems include:

-Gas Turbines with Heat Recovery: Systems that use a gas turbine to generate electricity, with the exhaust heat recovered to produce steam or hot water.

-Steam Turbines with Heat Recovery: Systems where steam produced in a boiler generates electricity in a steam turbine, and the exhaust steam is used for heating or industrial processes.

-Combined Cycle Systems: These combine gas turbines and steam turbines for enhanced efficiency. Waste heat from the gas turbine generates steam, which drives a steam turbine for additional power generation. **[3]**

3.2.4 Heat exchangers

Heat exchangers are most commonly used to transfer heat from the combustion exhaust gas. Since natural gas enters a boiler at a lower temperature, less energy must be supplied by the fuel. To predict the performance of a heat exchanger, it is essential to relate the total heat transfer rate to such quantities as the input and output fluid temperatures, the overall heat transfer coefficient, and the total heat transfer area. Two of these relationships can easily be obtained by applying the overall energy balances for the hot and cold fluids, if $\dot{q}$ is the total heat transfer rate between the fluids (hot and cold), with negligible heat transfer between the exchanger and its surroundings, as well as the potential changes and kinetic energy are negligible, the application of the heat balance gives the following equations:

$$Q_h = \dot{q}_h \times \left(H_{in,h} - H_{out,h}\right) \qquad (1)$$

$$And$$

$$Q_c = \dot{q}_c\left(H_{in,c} - H_{out,c}\right) \qquad (2)$$

Where:

Q_h represents the heat transfer for the hot fluid in Joules (J).

$\dot{q}_h$ is the heat transfer rate for hot fluid in Watts (J/s)

$H_{in,h}$ denotes the enthalpy at the inlet for the hot fluid in Joules per kilogram $\left(\frac{\text{J}}{\text{kg}}\right)$.

$H_{out,h}$ denotes the enthalpy at the outlet for the hot fluid in Joules per kilogram $\left(\frac{\text{J}}{\text{kg}}\right)$.

Q_c represents the heat transfer for the cold fluid in Joules (J).

$\dot{q}_C$ is the heat transfer rate for cold fluid (J/s)

$H_{in,c}$ denotes the enthalpy at the inlet for the cold fluid in Joules per kilogram $\left(\frac{\text{J}}{\text{kg}}\right)$.

$H_{out,c}$ denotes the enthalpy at the outlet for the cold fluid in Joules per kilogram $\left(\frac{\text{J}}{\text{kg}}\right)$.

If the liquids are not undergoing a phase change and constant specific heats are assumed, these expressions reduce to:

$$Q = \dot{q}_h Cp_h(T_{in} - T_{out}) \qquad (3)$$

$$And$$

$$Q = \dot{q}_c Cp_c(T_{out} - T_{in}) \qquad (4)$$

With:

Cp_h is the specific heat capacity of the hot fluid in Joules per kilogram per degree Celsius (J/kg°C)

Cp_c is the specific heat capacity of the cold fluid in Joules per kilogram per degree Celsius (J/kg°C).

Where the temperatures appearing in the expressions refer to the average fluid temperatures at the designated locations.

Note that the equations are independent of the flow arrangement and type of heat exchanger.

Another useful expression can be obtained by relating the total heat to the temperature difference transfer rate ΔT between the hot and cold fluids, where:

$$\Delta T = T_h - T_c \qquad (5)$$

An expression like this would be an extension of Newton's cooling law, with the overall heat transfer coefficient U used instead of the single convection coefficient h. However, ΔT varies with position in the heat exchanger, so it is necessary to work with an equation of the following form:

$$Q = US\Delta T_{LM} \qquad (6)$$

U is the overall heat transfer coefficient in Watts per square meter per degree Celsius (W/m²°C)

S is the heat transfer area in square meters (m²).

Where ΔT_{LM} is the logarithmic mean temperature difference (°C)

$$\Delta T_{LM} = \frac{\Delta T_2 - \Delta T_1}{\log\left(\frac{\Delta T_2}{\Delta T_1}\right)} \qquad (7)$$

Where ΔT_1 *and* ΔT_2 are the terminal temperature differences.

3.2.5.1 Co-current heat exchanger

The temperature distributions of hot and cold fluids associated with a parallel stream heat exchanger are shown in Figure 6 below.

The temperature difference ΔT is initially large but decreases rapidly with increasing x, asymptotically approaching zero. It is important to note that, for such an exchanger, the outlet temperature of the cold fluid never exceeds that of the hot fluid.

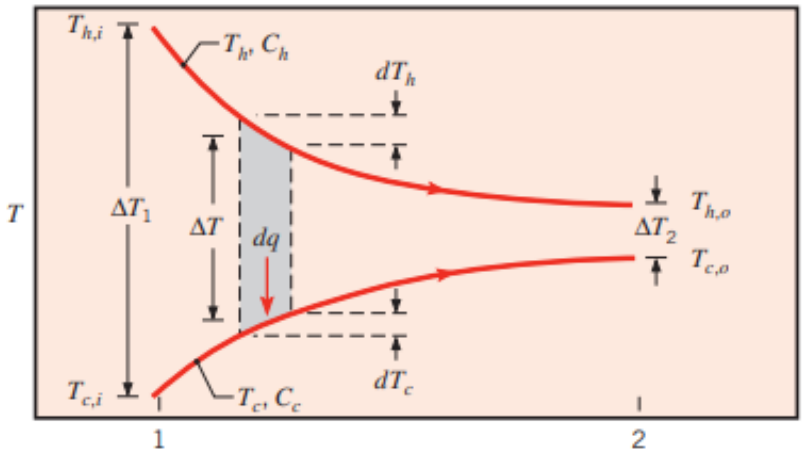

Figure 6. Temperature distribution in a parallel co-current exchanger.[6]

3.2.5.2 Countercurrent heat exchanger

The hot and cold fluid temperature distributions associated with a counterflow heat exchanger are shown in Figure 7. In contrast to co-current exchanger, this configuration allows heat transfer between the hot portions of the two fluids at one end and between the colder portions at the other.

For this reason, the variation in temperature difference, $\Delta T = T_h - T_c$ compared to x is nowhere as great as for the inlet region of co-current exchanger. Note that the outlet temperature of the cold fluid may now exceed the outlet temperature of the hot fluid.

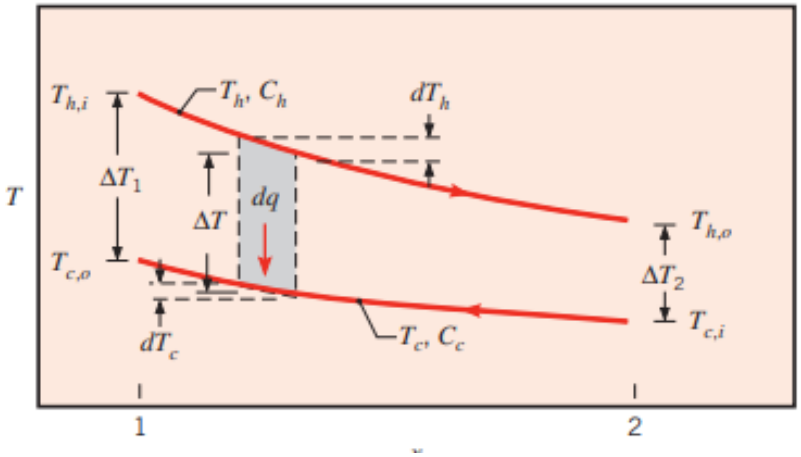

Figure 7. Temperature distribution in a countercurrent exchanger.[6]

Note that, for the same inlet and outlet temperature, the average temperature difference intended for countercurrent is greater than that for parallel flow. Therefore, the specific surface area is required to perform a prescribed q at the heat transfer rate is smaller for the counterflow than for the parallel flow arrangement, assuming the same value of U. Also note that can $T_{h,in}$exceeds $T_{c,out}$ for countercurrent, but not for co-current.

3.2.5.3 Special operating conditions

It is useful to note some special conditions under which heat exchangers can be operated. The temperature distributions for a heat exchanger in which the hot fluid has a thermal flow rate $C_h = \dot{m}_h Cp_h$ is much larger than that of the cold fluid $C_c = \dot{m}_c Cp_c$. For this case, the temperature of the hot fluid remains approximately constant throughout the heat exchanger, while the temperature of the cold fluid increases. The same condition is realized if the hot fluid is condensing vapor. Condensation occurs at a constant temperature, and for all practical purposes.

3.2.5.4 Calculation of heat flow in exchanger

Under these conditions, the heat flow $d\phi$ transmitted from the hot fluid to the cold fluid through element dS will be written, in the case of the co-courant exchanger:

$$d\phi = -\dot{m}_h Cp_h\left(T_{h,in} - T_{h,out}\right) = \dot{m}_c Cp_c\left(T_{c,out} - T_{c,in}\right) \qquad (8)$$

a. Co-current exchanger

$\dot{m}_h$ and $\dot{m}_c$ are the respective mass flow rates of hot and cold fluids, in *kg/s*. Cp_h and Cp_c are their heats of mass at constant pressure, in *J/kg °C*.

$$dT_h = -\frac{d\phi}{\dot{m}_h Cp_h} \quad and \quad dT_c = \frac{d\phi}{\dot{m}_c Cp_c} \qquad (9)$$

Hence the difference:

$$dT_h - dT_c = d(T_h - T_c) = -\left(\frac{1}{\dot{m}_h Cp_h} + \frac{1}{\dot{m}_c Cp_c}\right) d\phi$$

$$d(T_h - T_c) = -\left(\frac{1}{\dot{m}_h Cp_h} + \frac{1}{\dot{m}_c Cp_c}\right) k(T_h - T_c) dS \rightarrow \frac{d(T_h - T_c)}{T_h - T_c} = -\left(\frac{1}{\dot{m}_h Cp_h} + \frac{1}{\dot{m}_c Cp_c}\right) k\, dS$$

(10)

Assumption: k=constant along the exchanger ➔ integration of (6) Entropy (in this context, it likely represents the change in entropy from an initial state where S=0S to a final state S).

$$[Log(T_h - T_c)]_{S=0}^{S} = -\left(\frac{1}{\dot{m}_h Cp_h} + \frac{1}{\dot{m}_c Cp_c}\right) k\, S \qquad (11)$$

- ✓ At the exchanger inlet *(x=0)* $T_h - T_c = T_{hin} - T_{cin}$
- ✓ At the outlet of the exchanger *(x=L)* $T_h - T_c = T_{hout} - T_{cout}$

$$(7) \rightarrow Log\frac{T_{h,in} - T_{c,out}}{T_{h,in} - T_{c,in}} = -\left(\frac{1}{\dot{m}_h Cp_h} + \frac{1}{\dot{m}_c Cp_c}\right) k\, S \qquad (12)$$

But we can also express the total flow exchanged as a function of the inlet and outlet temperatures of the fluids; it is to make the global enthalpic balance of each fluid, which is written:

$$\phi = \dot{m}_h Cp_h\left(T_{hin} - T_{h,out}\right) = \dot{m}_c Cp_c\left(T_{c,in} - T_{c,out}\right) \quad (13)$$

$$(8)\ and\ (9) \rightarrow Log\frac{T_{h,out} - T_{c,out}}{T_{h,in} - T_{c,out}} = -\left(\frac{(T_{h,in} - T_{h,out})}{\phi} + \frac{(T_{c,out} - T_{c,in})}{\phi}\right) k\, S$$

$$= \left[(T_{h,out} - T_{c,out}) - (T_{h,in} - T_{c,in})\right]\frac{kS}{\phi} \quad (14)$$

Expression from which we finally get the total thermal power exchanged, assuming a circulation with parallel flows:

$$\phi = k\,\frac{(T_{h,out} - T_{c,out}) - (T_{h,in} - T_{c,in})}{Log\frac{T_{h,out} - T_{c,out}}{T_{h,in} - T_{c,in}}}\, S \qquad (15)$$

b. Countercurrent exchanger

The temperature change dT_c of the cold fluid when increasing the exchange area by dS, becomes negative. Under these conditions, the total heat power exchanged is written:

$$\phi = k\ \frac{(T_{h,in} - T_{c,out}) - (T_{h,out} - T_{c,in})}{Log\frac{T_{h,out}-T_{c,out}}{T_{h,out}-T_{c,in}}}\ S \qquad (16)$$

3.2.5.5 Heat exchanger efficiency

The efficiency of a heat exchanger is the ratio of the thermal power actually exchanged to the maximum exchange power theoretically possible, with the same conditions of entry of the fluids (nature, flow fluids (nature, flow rate...) in the exchanger.

$$\varepsilon = \frac{\phi_{real}}{\phi_{max}} \quad (17)$$

ϕ_{max} : one of the two fluids undergoes a temperature change equal to the maximum temperature gradient existing in the device. This maximum heat transfer flow is obtained when one of the fluids (lower thermal capacity) exits at the inlet temperature of the other.

Consider $C_c > C_h$➔The hot fluid controls the transfer.

$$\phi_{real} = C_h(T_{h,in} - T_{h,out}) = C_c(T_{c,out} - T_{c,in}) \quad (18)$$

For S ➔∞, we obtain: $\phi_{max} = C_h(T_{h,in} - T_{c,in})$ (19)

Cooling efficiency:$\varepsilon = \frac{T_{h,in}-T_{h,out}}{T_{h,in}-T_{c,in}}$ (20)

In countercurrent, ε we can reach 1 $\forall C_h\ and\ C_c$. However, In Co-courant, the efficiency is limited by the relative value C_c/C_h

The output temperature with ➔∞ is:

$$T_{out} = \frac{(C_h T_{h,in} + C_c T_{c,in})}{(C_h + C_c)} \quad (21) \qquad thus \qquad \varepsilon = \frac{C_c}{C_h + C_c} \quad (22)$$

➔ If $C_h/C_c = 1$➔$T_{out} = \frac{T_{h,in}+T_{c,out}}{2}$ and $\varepsilon = \frac{1}{2}$

➔ If C_h/C_c➔0 so $T_{out} \approx T_{c,out}$ and $\varepsilon = 1$

If $C_c < C_h$ the cold fluid controls the transfer

$$\phi_{max} = C_c(T_{hin} - T_{cin}) \quad (23)$$

Heating efficiency $\boxed{\varepsilon = \frac{T_{c,out} - T_{c,in}}{T_{h,in} - T_{c,in}}}$ (24)

3.2.5.6 Number of transfer unit (NTU)

The transfert of unit, NTU reflects the relationship between the heat exchanger's characteristics and its performance. The NTU is indeed a dimensionless parameter that measures the effectiveness of a heat exchanger. It's defines as :

$$NTU = \frac{kS}{C_{min}}$$

Assume $Z = \frac{C_h}{C_c} < 1 \quad and \quad \Delta T_{max} = T_{h,in} - T_{h,out}$ (25)

$$NTU = \frac{kS}{C_{min}} = \frac{kS}{C_h} = \frac{T_{h,in} - T_{h,out}}{\Delta T_2 - \Delta T_1} \quad (26)$$

Let's define ΔT_1 and ΔT_2 in terms of ΔT_{max} and ε. Then we can write:

$$\Delta T_2 = T_{h,out} - T_{c,in} = \left(T_{h,out} - T_{h,in}\right) + \left(T_{h,in} - T_{c,in}\right) = -\varepsilon \Delta T_{max} + \Delta T_{max} = \Delta T_{max}(1 - \varepsilon) \qquad (27)$$

$$\Delta T_1 = T_{h,in} - T_{c,out} = \left(T_{h,in} - T_{h,out}\right) + \left(T_{h,out} - T_{c,out}\right) = \Delta T_{max} - Z\left(T_{h,in} - T_{h,out}\right) = \Delta T_{max}(1 - Z\varepsilon) \qquad (28)$$

Let's consider the case of a simple tubular exchanger operating in countercurrent and assume that the hot fluid drives the transfer $C_c > C_h$ ($C_{min} = C_h$):

We therefore deduce the relationship between NTU and the efficiency.

$$NTU = \frac{T_{h,in} - T_{h,out}}{\Delta T_2 - \Delta T_1} = \frac{\varepsilon \Delta T_{max}}{\Delta T_{max}(1 - \varepsilon) - \Delta T_{max}(1 - Z\varepsilon)} log\left(\frac{\Delta T_{max}(1 - \varepsilon)}{\Delta T_{max}(1 - Z\varepsilon)}\right) \quad (29)$$

$$\boxed{NTU = \frac{1}{1-Z} log\left(\frac{(1-Z\varepsilon)}{(1-\varepsilon)}\right) \qquad (30)}$$

Although the flow conditions are more complicated in multi-pass and cross-flow heat exchangers, the equations can still be used if the following modification is made to the log mean temperature difference.

$$\Delta T_m = F \Delta T_{m,CF} \qquad (31)$$

In other words, the appropriate form of $\Delta T_m$is obtained by applying a correction factor to the value of ΔT_m that would be calculated under the assumption of countercurrent conditions.

Algebraic expressions for the correction factor F have been developed for different tubes and cross-flow heat exchanger configurations, and the results can be represented graphically.

3.2.5.7 Fouling in heat exchanger

Fouling is a complex phenomenon where material deposits form on heat exchanger surfaces, significantly reducing performance by increasing thermal resistance. It is influenced by variables such as the heat exchanger design, operating conditions, surface properties, and fluid characteristics. The fouling process involves transport initiation, fixation, removal, and aging. Despite research efforts, predicting fouling accurately is challenging. Therefore, heat exchanger designs incorporate a constant fouling factor, R_f to account for decreased efficiency due to fouling, with different fluids exhibiting varying fouling resistances. (see Appendix 1).

3.2.5.8 Heat exchanger selection

Shell and tube exchangers are designed for virtually any capacity and operating conditions, from high vacuum to ultra-high pressure, from cryogenics to high temperatures, and for temperature and pressure differences between fluids, limited only by the materials of construction. They can be designed for special operating conditions: vibration, heavy soiling, highly viscous fluids, erosion, toxicity, radioactivity, multi-component mixtures, etc. They are manufactured from a variety of metallic and non-metallic materials. They generally have an order of magnitude surface area per unit volume than compact heat exchangers, and require considerable space, weight, support structure and footprint.

From an operation and maintenance perspective, compact heat exchangers are utilized for specific applications such as high-temperature applications (up to approximately 850°C or 1550°F), high-pressure applications (over 200 bar), and moderate fouling applications. However, these applications do not typically involve both high-temperature and high-pressure conditions simultaneously.

Fouling is one of the main potential problems in many compact heat exchangers, except for plate heat exchangers. With a large face-to-face exchanger, poor flow distribution could be another problem. Due to short transient times, careful design of controls is required for the start-up of some compact heat exchangers with shell-and-tube heat exchangers. No industry standards or recognized practices for compact heat exchangers is yet available.

3.3 General information on combustion

Combustion is an exothermic chemical oxidation reaction. It can only occur if three elements come together: a fuel, an oxidizer and sufficient activation energy in sufficient quantities. The chemical reaction is written as follows:

Fuel + Oxidizer → Combustion Products + Heat

The oxidizer is atmospheric air whose composition is as follows:

Table 5. Air composition

	% in Mass	% in Volume
O_2	24	21
N_2	76	79

Combustion products (fumes) consist mainly of carbon dioxide, nitrogen and water vapor, while Sulphur oxide, carbon monoxide and other solid or gaseous unburnt substances may also be present. The presence of fuel, air and a spark are not enough to achieve good combustion: depending on the quantity of air, the settings of the combustion appliance, the chimney...etc., combustion will be of more or less "good" quality, without toxic products for humans or the environment in the smoke, and with good efficiency. **[5]**

3.3.1 Advanced Combustion Analysis and Practical Calculations

The fundamental difference between this section and the first part of the course lies in the complexity of the fuels we use in the real world, which are far from being representable as simply as by the formula $CxHy$. We will therefore begin by taking a look at the fuels used today. Then we'll learn how to calculate the composition of combustion products of combustion for a complex fuel to determine the flue gas losses (chemical and thermal). We'll then look at the problems of pollution caused by emissions, and we'll finish by studying the phenomenology of combustion end with a study of combustion phenomenology in general and in boilers, furnaces and boilers, furnaces and engines.

3.3.1.1 Complex fuel (natural gas)

Fuels can come from a wide variety of sources and contain varying quantities of useful elements: carbon and hydrogen, and neutral or even harmful elements: oxygen, nitrogen, sulfur, minerals (which turn to ash) ...

To calculate the composition of their fumes, we need to know their chemical composition. They are classified below according to their nature:

Natural gas is a fuel that comes from deep within the earth. It is composed of over 80% methane (CH_4) which is colorless and odorless, and is the simplest hydrocarbon found in

nature. Methane is also produced on the earth's surface during fermentation processes under anaerobic conditions, notably in marshes, sewage treatment plants or livestock farms (biogas).

3.3.1.2 Calorific value

When combustion is not stoichiometric, it can be defined in several ways, usually by its excess of air, or its deficiency of air, or by the richness R, or its inverse the air factor λ. The excess air is the percentage of excess air compared to the stoichiometric reaction. The richness R is defined as the ratio of the number of moles of fuel contained in a given quantity of mixture to the number of moles of fuel contained in the stoichiometric mixture. From these definitions, the equivalence results:

$$R = \frac{1}{1+e} \quad (32)$$

e is the excess air fraction (e.g., e=0.2 means 20% excess air).

The calorific value of a fuel is the quantity of heat released by complete combustion under normal atmospheric pressure.

- Calorific Value of Fuel

The calorific value (or heating value) of a fuel is the amount of heat released during the complete combustion of a specified amount under standard conditions.

Higher Heating Value (HHV): The total heat released when the fuel is completely burned and the products have returned to the initial temperature of the reactants, including the latent heat of vaporization of water.

Lower Heating Value (LHV): The heat released when the fuel is completely burned, but the products are allowed to escape as gases, not condensing the water vapor.

3.3.1.3 Calculation of the combustion power of complex fuel

It designates the strictly necessary and sufficient quantity of air that must be supplied to ensure neutral combustion of the fuel unit.

$$V_a = \frac{V_{O_2}}{\%O_2\ by\ air\ volume} = \frac{V_{N_2}}{\%N_2\ by\ air\ volume} \quad (33)$$

Where :

V_a Total volume of air in cubic meters m^3

V_{O_2} Total volume of oxygen in cubic meters m^3

V_{N_2} Total volume of nitrogen in cubic meters m^3

One mole of carbon dioxide requires one mole of oxygen to form, as does SO_2. Water, on the other hand, requires half a mole of oxygen. The quantity of oxygen required is therefore the sum of these three quantities. Subtract the amount of oxygen contained in the fuel to obtain the quantity of oxygen contained in the oxidizer. And to get the full amount of divide the oxygen content of the oxidizer by ψ.

$$V_a = \frac{1}{\psi}\left(V_{CO_2} + V_{SO_2} + \frac{V_{H_2O}}{2} - V_{O_2}\right) \qquad (34)$$

Ψ =0,21 for air, between 0,21 and 1 for certain industrial applications with over-oxygenated air and 1 for oxygen.

3.3.1.4 Smoke powers

This is the quantity of smoke produced by the neutral combustion of a unit of fuel.

There are two types of smoke power:

- ✓ Dry Smoke power

We add the volume of the various gases contained in the fumes, excluding water vapor.

$$V_{DS} = V_{CO_2} + V_{SO_2} + V_{N_2} + (1 - \psi)V_a \qquad (35)$$

The nitrogen comes from the fuel V_{N_2} and the oxidizer $(1 - \psi)V_a$ which is the volume of nitrogen resulting from the neutral combustion of the quantity of air Va.

- ✓ Wet Smoke power

$$V_{WS} = V_{DS} + V_{H_2O} + V_H \qquad (36)$$

Water vapor comes from combustion: V_{H_2O} and from the moisture in the fuel: V_H is the volume of water vapor produced by the moisture in the fuel.

3.3.1.5 Accurate calculation of smoke loss

<u>a. sensible heat loses</u>

- Integral calculation of the enthalpy of the flue gases and the fresh mixture sensible heat losses can be written as:

$$P_{th} = q_m\left(\int_{273}^{T_S} Cp_F dT - \int_{273}^{T_R} Cp_R dT\right) \qquad (37)$$

The R is intended for the mixture of "Reactants": oxidizing fuel before combustion.

Unless the oxidizer is preheated on the second term of the second member is very small, and can be calculated with sufficient accuracy by taking constant Cp_R equal to that of air 1 kJ/kg°C.

In general, the molar specific heats Cp' of different compounds are expressed in polynomial form. According to the authors, the expressions vary. One of the simplest is shown below.

For diatomic gases (O_2,N_2,CO…): $Cp' = 27{,}8 + 0{,}004\,T$

For steam $Cp' = 27{,}8 + 5{,}3.10^{-3}\,T + 4{,}9.10^{-6}T^2$ (38)

For carbon dioxide $Cp' = 27{,}8 + 33{,}4.10^{-3}\,T - 9{,}7.10^{-6}T^2$ (39)

Cp are in J/mole°K and T in K. To calculate Cp' of the mixture, multiply the $Cp'_i$of each constituent by its mole fraction and sum:

$$Cp' = \sum X_i Cp'_i \quad (40)$$

The average molar mass is calculated in the same way, and finally the mass Cp is the ratio of the molar Cp' to the molar mass:

$$Cp = \frac{Cp'}{M} \quad (41)$$

The molar mass of the flue gases is almost identical to that of air regardless of the fuel and excess air. There are other more precise relationships. **[7]**

A widely used semi-empirical formula is that of Siegert. It provides an accuracy of around 5% within the correct ranges of CO_2. It calculates the percentage of heat loss in relation to the *LHV* in the following form:

$$100\,\frac{q_{th}}{LHV} = \frac{K_S}{100\gamma_{CO_2}}(T_S - T_R) \quad (42)$$

With K_S= 0.47 for natural gas, 0.6 for medium hydrocarbons, 0.62 for heavy fuel oil and 0.71 for coal. Today's electrochemical analyzers are equipped with calculators which give the technician a direct value for these losses, calculated from the measurement of CO_2 and knowledge of the fuel.**[7]**

b. Latent heat losses

In most cases, water remains in vapor form in the flue gases, and its latent heat does not need to be its latent heat. The only case where it must be taken into account for the balance is in the case of natural gas condensing boilers. We calculate the maximum condensable water flow rate q_{mH2O} is calculated from the total hydrogen V_{H2O}.

$$q_{mH_2O} = q_{mc} V_{H_2O} \rho_{(H_2O)0} \quad (43)$$

Where q_{mc} is the fuel flow rate in (Nm^3/S) if it's a gas or kg in if it's a solid or a liquid. $\rho_{(H_2O)_0}$ is the density of water vapor under standard conditions:

$$\rho_{(H_2O)0} = \frac{18}{22{,}4} = 0{,}8036\ kg/Nm^3 \qquad (44)$$

Latent heat losses can therefore be written as:

$$P_{LV} = \left(q_{mH_2O} - q_{mcond}\right) Lv_{H_2O} \qquad (45)$$

Where q_{mcond} is the condensed water discharge and $Lv_{H_2O} = 2500 kJ/kg$.

In the following figure 8, $Q_{LV} = q_{mH_2O} Lv_{H_2O}$ means the maximum latent heat loss (without condensation) as a function of the molar ratio condensation) as a function of the fuel's H/C molar ratio.

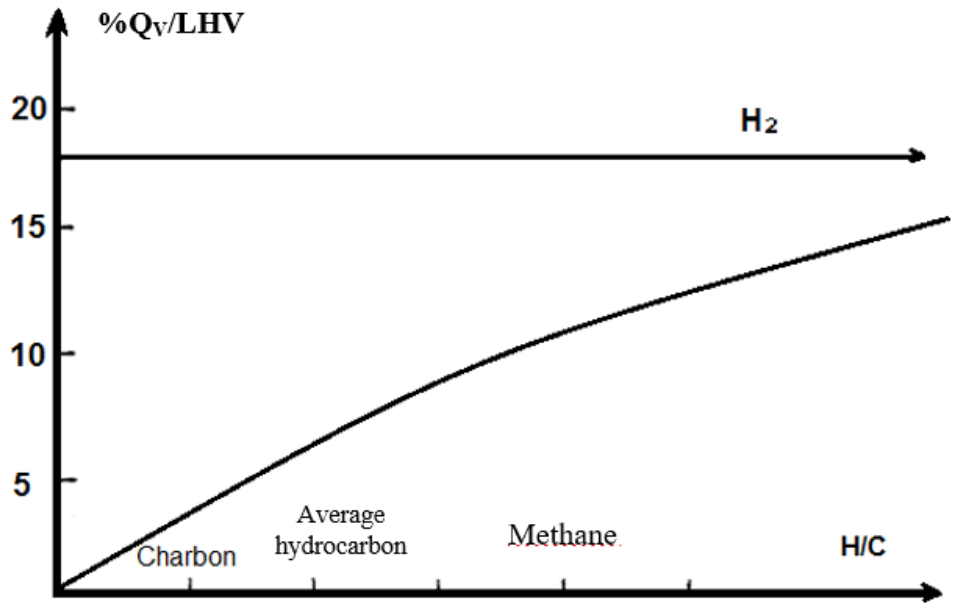

Figure 8. Latent heat losses [7]

Pollutant reduction and regulatory limitations

The causes of pollution by engine or thermal installations are multiple. They present an 'inevitable' nature when the pollutant emitted is due to the composition of the fuel, such as:

- sulfur in fuels producing SO2,
- organometallic compounds in coals producing fly ash,
- or chlorine in the incineration of waste...

It's pointless trying to eliminate them by acting on combustion. Other pollutants such as CO, NO, soot... are largely dependent on machine design or adjustment.

- Ashes: these are inherent to the fuel. Their emission can only be reduced by filtration. Modern electrostatic filters are over 99% efficient. The regulations impose a maximum threshold of 129 mg/kWh.
- Solid unburned particles: In the form of black smoke giving soot, the presence of solid unburned particles reveals a mixing problem. They come from the cracking of the fuel in the gaseous or liquid phase. They are very difficult to eliminate during the combustion of heavy fuels. The legal threshold is 215 mg/kWh.

3.4 Thermodynamic properties of reacting species

Understanding the thermodynamic properties of reacting species is essential in studying combustion, as it helps determine the energy exchanges that occur during chemical reactions. The key properties to consider are internal energy and enthalpy, which provide insights into the energy changes from the reactants to the products.

3.4.1 Internal Energy and Enthalpy :

Internal Energy (U): This is the total energy contained within a system, including the kinetic and potential energies of the molecules. It is particularly relevant for calculating energy exchanges in reactions occurring at constant volume.

Enthalpy (H): Enthalpy is the measure of the total heat content of a system, including internal energy plus the product of pressure and volume. It is used for reactions occurring at constant pressure, such as many combustion processes.

3.4.2 Heat of Reaction: The heat of reaction, or the change in enthalpy, represents the heat absorbed or released during combustion. This value depends on the conditions under which the reaction occurs:

Constant Volume: The heat of reaction corresponds to the change in internal energy.

Constant Pressure: The heat of reaction corresponds to the change in enthalpy.

3.4.3 Application in Combustion Analysis:

Energy Exchanges: By understanding the internal energy and enthalpy of reactants and products, we can calculate the total energy released or absorbed during combustion. This information is crucial for designing efficient combustion systems and evaluating fuel performance.

Combustion Efficiency: Comparing the energy released during actual combustion to the theoretical maximum helps in optimizing fuel usage, improving efficiency, and reducing waste.

Environmental Impact: Knowledge of energy exchanges allows for better prediction and control of pollutant formation. By adjusting combustion conditions, we can minimize emissions of harmful byproducts like NOx, CO, and unburned hydrocarbons.

Heat of Formation: The heat of reaction can be linked to the heats of formation of the reactants and products, providing a detailed understanding of the energy involved in forming each compound from its elements.

4. System modeling

4.1 Introduction

The purpose of this chapter is to technically study a turbogenerator and its auxiliaries, taking into account all the information provided in the previous chapters and considering the conditions in which our PRS operates as well as the characteristics of the fuel passing through this station. Our theoretical sizing concerns heat exchangers forming an intermediate circuit between a preheater and a heat source. We have chosen a heat source to feed the gas preheater based on the statistics obtained in advance through our study.

4.2 Natural gas pressure-reducing station

The PRS gas pressure regulator station provides filtration, heating, pressure reduction and gas metering.

There are two PRS in the central plant, the first common to both units (3 and 4), each supplying a boiler. Each boiler has its own pressure-reducing line, and three identical lines installed in parallel are capable of providing 120% of the flow required to operate a boiler. An additional expansion line is provided as a reserve. Maintenance operations can therefore be carried out on the reserve line, after purging the equipment with nitrogen.

4.2.1 General system description and operation

The natural gas is delivered to the expansion station via a pipeline at a pressure of between 15 and 20 bar, where it passes through a separator to rid it of liquid particles, then divides into three ramps where there are three filters designed to rid the gas of solid particles, and through three heaters, one in each ramp, the gas undergoes an increase in its temperature, the aim being to avoid the risk of icing up the equipment caused by the pressure drop at the expansion valves. After expansion, a metering system measures the flow consumed to provide accurate information to the plant control room.

The gas pressure regulator station (see Appendix 3) comprises the following main components:

- A primary liquid separator (common to all three lines)
- Three filters
- Three heaters
- Three regulators
- Three counter stations
- Control and measurement equipment required for operation

- Manual piping and valves
- Pneumatic shut-off valve
- Control valves
- Safety valve
- Nitrogen purge valve connections and vents

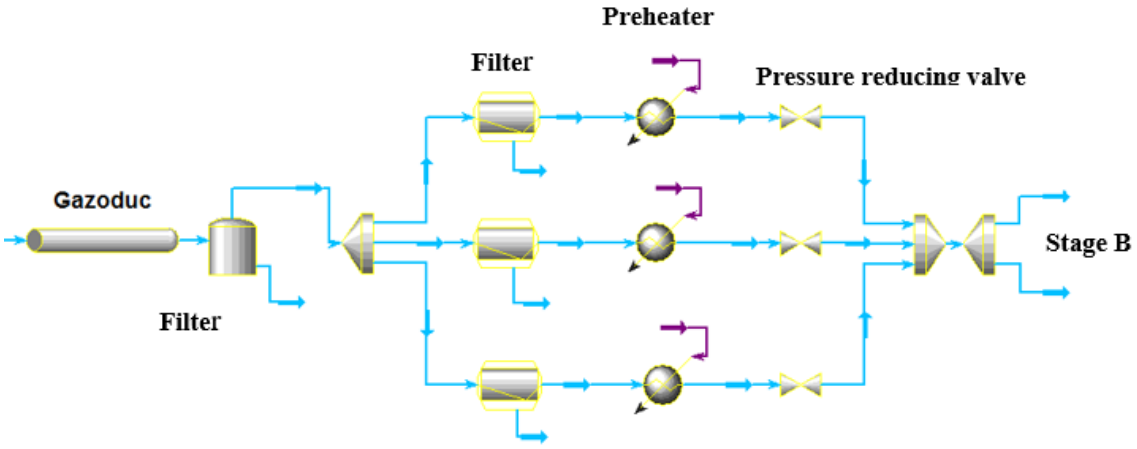

Figure 9. PRS installation diagram [8]

The supply includes the package circuit from the dielectric seal upstream of the PRS to the common manifold for the three expansion lines and the two boiler feed branches.

After the liquid separator at the station inlet for each line, the gas is delivered to the filter designed to rid the gas of suspended solids and to the reheating system (gas temperature: inlet 15°C - outlet 35°C). After reheating, the gas pressure is reduced from 15-20 bars to 4.6 bar for the expansion system. After expansion, a metering system with temperature and pressure correction measures the flow rate consumed.

4.2.2 Technical description of the supply

a. Dielectric seal

A dielectric joint upstream of the PRS is designed for a 10" diameter pipe, and two joints at the PRS outlet are designed for a 14" diameter pipe.

b. Input isolation valve

A manual 10" isolation ball valve controlled by the local control room and by the INFI 90 system in the remote-control room. The pneumatic valve is located downstream of the manual isolation valve and upstream of the liquid separator bypass.

c. Separator

A liquid separator, designed to remove suspended liquids such as water, light or heavy oils, etc., from the gas it may carry, with isolation valve and bypass valve of the ball type. The separator is designed based on the principle of stainless-steel lamella pack separation, for a maximum gas flow rate of 102,000 Nm^3/h and a separation efficiency of 99% with liquid particles of 5 μ. The gas composition is not always the same: when there is no gas in equilibrium with the condensates (for example at 15°C and 20 bar), there are also no condensates removed in the separator, but it is always necessary to ensure that there are condensates in the tank to provide the "liquid seal" on the drain pipe of the lamella pack. Before start-up, a liquid leg (hydrocarbons and/or water) must be provided to ensure the "liquid seal". The separator is equipped with vent valves and safety valves which discharge into the line to the existing high torch. Periodic maintenance of the safety valve, as well as maintenance of the separator itself, is carried out using the bypass pipe. The separator is provided with a sight glass level gauge and four level switches: very high, high, low, and very low. The high and low levels open and close the drainage valve in relation to the gained level. When the low level does not intervene, it is the very low level that closes the drainage valve. The very high and very low levels are signaled as alarms in the remote-control room (INFI 90 system). The same INFI 90 system manages the logic of opening and closing the drainage valves.

d. Filters

Three filters, one for each pressure relief line, designed to remove solid particles suspended in the gas that it may carry. Each filter is designed based on the principle of fiberglass cartridges, with a filtration efficiency of 99% for particles of 0.5 μ. A pneumatic isolation valve is provided for each filter and managed in opening and closing by the control room. Each filter is equipped with a vent valve and safety valve common to the heaters, which discharge into the line to the existing high torch. Each filter is equipped with a differential pressure gauge with local indication and alarm signal. The purge valve is pneumatically actuated by the normal drainage level and connected to the purge collector. The filter is designed as a pressure vessel and in accordance with the specifications sheet data. Each filter is provided with a sight glass level gauge and three level switches: high, low, and very high. The high and low levels open and close the drainage valve in relation to the gained level. The very high level is signaled by an alarm in the control room.

e. Heating units

Three gas reheaters, one for each expansion line. Each reheater is fitted with a trap for condensed steam, and is designed for maximum throughput for each boiler, to prevent icing during downstream expansion operations.

The reheating fluid is steam from the secondary steam circuit at 180°C and 8 bar pressure. Each U-tube horizontal reheater is fitted with a vent valve and safety valve (common to all filters), which vent into the line towards the high flare. The corrosion allowance on these heat exchangers is 3.2mm.

Table 6. Existing heater characteristics. (see Appendix 4)

Heat exchanged 380000 kcal/h	**Gas side**	**Vapor side**
Flow	50 000 Nm^3/h	658 kg/h
Pressure	18-22 bar	8 bars
Temperature (in/out)	0/20°C	180/90°C
Study pressure	30 bars	12 bars
Study temperqture	50°C	250°C
Bride classes	300#	300#

g. Line shut-off valves

Three safety shut-off valves, one for each expansion line, are provided upstream of the regulators. Each valve is activated and closed pneumatically to interrupt the supply of fuel gas; the signal being received from the gas pressure when the value downstream of the regulator rises to 7.5 bar. The valve is opened manually. The valve is fitted with a safety lock in the closed condition.

h. Pressure regulators

Three primary expansion stations, one for each expansion line, are fitted with the expansion valves required for operation at all flow rates. The regulating valves are controlled by a local controller. The position of the valves is indicated on the control room system.

Downstream of each pressure-reducing valve, a safety valve is installed to vent the line to the existing high flare.

i. Metering station

Three turbine metering stations, one for each expansion line, are provided with temperature and pressure correction, enabling measurement of the flow rate consumed. The signals from the three turbines are sent to a computer installed in the local control room.

j. Isolation valve

Three isolation valves, one for each expansion line. Each manual ball-type isolation valve is provided at the outlet end of the line to isolate the line (there is also an isolation valve at the inlet end).

k. Output isolation valves

Two pneumatic isolation valves, each on a boiler feed branch, are controlled from the control room.

l. Outlet purge valves

Two pneumatic vent valves, each on a boiler supply branch, are provided downstream of the pneumatic outlet isolation valves to allow the pipe section downstream of the isolation valves to be cleared. The vent valve is controlled together with the isolation valve by the same signal.

m. Purge

Sufficient connections and valve vents are provided to allow the gas system to be purged with inert gas (such as nitrogen) and checked either after installation or for subsequent maintenance.

n. Control system

The PRS is controlled from the remote-control room (INFI 90 system). Local measurements are taken on the substation for pressure and temperature indications in the various parts of the installation. A frame is installed in a local control room located about 30 m from the substation.

The frame features:

- pushbuttons and signals for opening/closing the station's inlet and outlet valves. A selector switch allows the above-mentioned valves to be managed from the local control room, or from the INFI 90 system in the remote-control room.

- a calculator for indicating gas flow rates calculated according to pressure and temperature. Alarms relating to calculator malfunctions are sent to the INFI 90 system in the remote-control room.

4.3 Simple recovery of expansion energy by a turbogenerator

Turbogenerators are used to recover expansion energy in several countries around the world (Italy, Holland, France, etc.). A gas pipeline is equipped with compressor stations, which are the site of a major expansion in the gas skid, supplying fuel gas, instrument gas and motor

gas. This expansion energy can be recovered by adding turbogenerators. In this chapter, we will study the cost-effectiveness of installing a turbogenerator in the Stage B natural gas substation.

4.3.1 Turbogenerator functionality

The turbogenerator directly combines a gas expansion turbine (expansion without combustion) with an alternator, all in a single enclosure (housing), with no seals between moving parts as shown in figure 10.

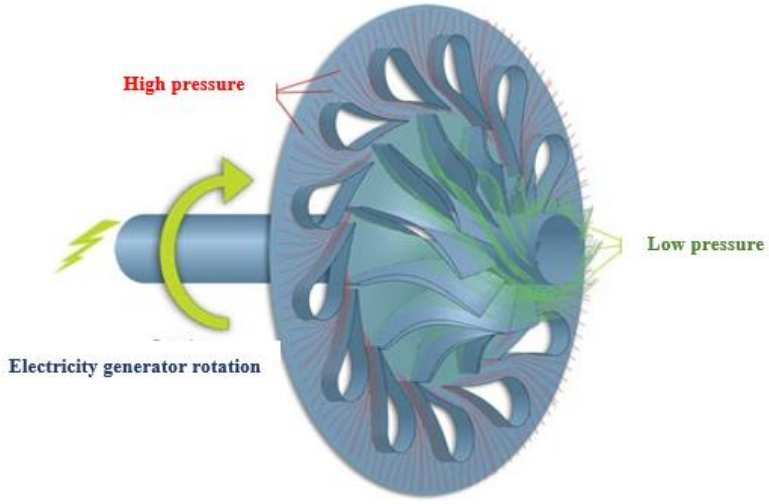

Figure 10. Radial reaction turbine. [9]

As the alternator rotates at the speed of the turbine mounted at the end of the shaft, the speed reducer is no longer necessary. The use of magnetic bearings eliminates all contact between the rotating and stationary parts, eliminating lubrication, wear and associated loss of efficiency, and making maintenance virtually non-existent.

Furthermore, whereas conventional systems are very noisy, the noise level of the magnetic-bearing turbogenerator remains very low due to the elimination of any source of mechanical vibration. With this technology, the turbine wheel mounted on the alternator rotor shaft no longer transmits its vibrations to the stator.

This level of energy recovery is designed for different flow rates, and is used in pressure-reducing stations.

Substations with higher flow rates can be equipped with several expansion turbines in parallel, and for higher upstream-downstream pressure ratios, these turbines are connected in series.

During expansion in these stations, the gas temperature drops by 0.4 °K/Bar (the Joule-Thompson effect). This cooling effect is accentuated by the fact that expansion takes place through a turbine, which extracts a large proportion of the gas's thermodynamic energy, and depends on the upstream/downstream pressure ratio. It is then necessary to heat the natural gas before expansion to avoid condensation and frosting. **[5]**

4.3.2 Energy balance of the system

Applying the Maxwell-Thomson-Gouy theorem, we obtain:

$$g.\Delta Z + C.\Delta C - W_m = \Delta H - T_0.\Delta S + Loss \quad (46)$$

Neglecting variations in kinetic energy and potential energy, this theorem translates into:

$$-W_m = \Delta H - T_0.\Delta S + Loss \quad (47)$$

Where:

g: Earth's gravitational acceleration. (m/s²)

T_0: Thermodynamic temperature. (k)

ΔC: Variation in kinetic energy. (J)

ΔZ: Variation in potential energy. (J)

W_m: Useful work supplied per unit mass of fluid. (J/kg)

$\Delta H = H_E - H_A$: Change in enthalpy of the unit mass of gas between exhaust and inlet of the expansion unit. (J/kg)

$\Delta S = S_E - S_A$: Change in entropy per unit mass of fluid. (J/kg)

$Loss$: Energy losses per unit mass of gas caused by all irreversibilities.

$\Delta H - T_0.\Delta S$: Corresponds to usable energy. (J/kg)

$T_0.\Delta S - pertes$: Corresponds to heat exchanges with the outside. (J/kg)

4.3.3Natural gas expansion in the turbine

This is expansion through a regulator-expander. This is characterized by an isenthalpic transformation ($\Delta H=0$). It is carried out by a laminating valve equipped with a Buse-clapet system. No work is exchanged with the outside ($W_m=0$).

At high pressure gradients, the outlet temperature can fall below the hydrate or condensate formation temperature, so preheating is required. **[10]**

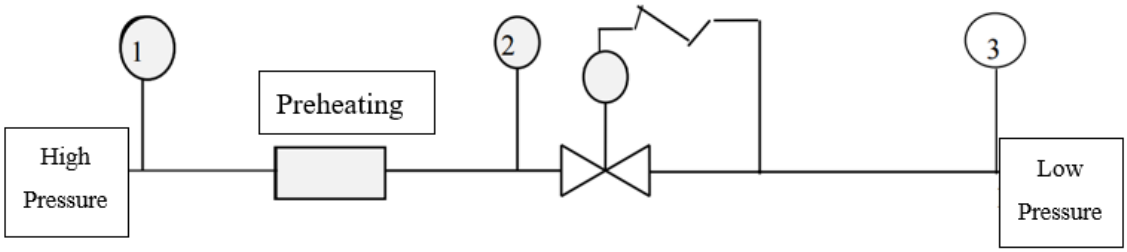

Figure 11. Simple PRS block Diagram.

- Transformation (1-2) corresponds to isobaric preheating.
- Transformation (2-3) corresponds to isenthalpic expansion.

Following the Maxwell-Thomson-Gouy formula, we note that we can carry out the same transformation from P_1 to P_2, by collecting work on the shaft of a machine. The work supplied by the unit mass of gas is equal to the enthalpy variation during the evolution:

$$-W_m = \Delta H \quad (48)$$

The evolution of the gas is represented on a *(P-H)* diagram as follows

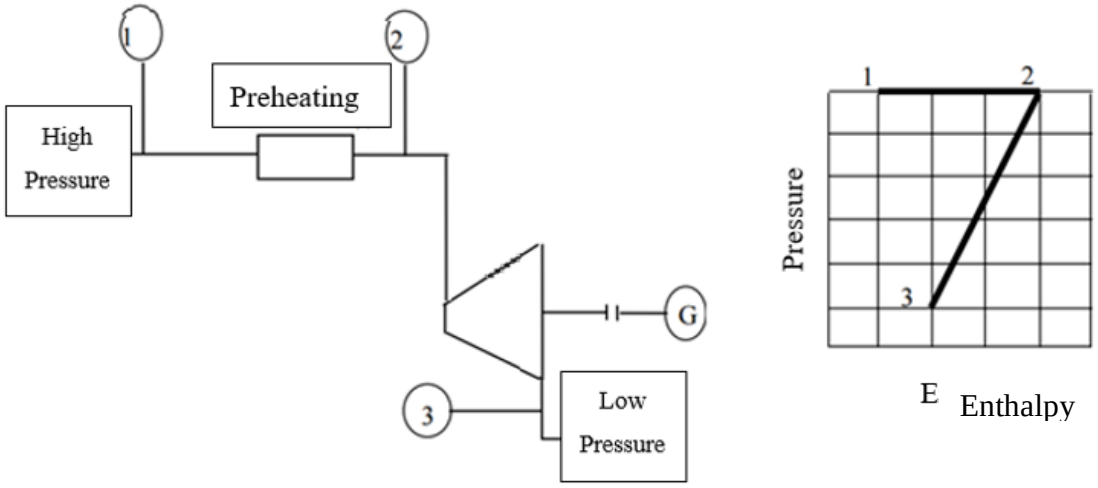

Figure 12. Gas evolution in the turbo-generator system. [10]

4.3.4 Condensate and hydrate formation

As the expansion in a turbine leads to significant drops in gas temperature, condensate or hydrates can form as a result. Therefore, initially, we investigated the conditions under which the turbogenerator can operate safely for both personnel and installations. Several simulations were conducted using calculation software to determine the dew point temperature of natural gas. The results obtained are shown in Table 7. **[11]**

Table 7 displays the dew point temperatures as a function of pressure. It is evident that these temperatures are very low, making condensate formation very difficult. On the other hand, calculations of the temperature for hydrate formation were carried out using the solid-vapor equilibrium curves of natural gas (see Appendix 2). The value obtained is 10°C. **[11]**

Table 7. The Dew-point temperature calculation.

Pressure (atm)	Dew-point temperature (°C)
5	-74.87
10	-67.01
15	-62.69
20	-60.01
25	-58.34
30	-57.39
35	-57.04
40	-57.25
45	-58.07
50	-59.69
55	-63.03

4.4 Sizing the Turbine

The objective of this project is to apply a modeling methodology to an industrial scientific problem concerning the generation of electricity from the pressure drop of the fuel (without combustion) before it is utilized by the steam cycle boiler. Initially, we will perform sizing through simple theoretical calculations to evaluate approximate results, which will guide us in modeling the various components of the desired system.

Firstly, we focus on the expansion work of the turbine, designed for various flow rates and relatively variable upstream-downstream pressure ratios. According to one of the fundamental principles of energy system design, we must consider the most unfavorable conditions for the operation of our system. For this purpose, we assume that the volumetric flow rate of natural gas taken by the boilers in step B has a minimum production of about 40,000 Nm3/h, and that the minimum gas inlet pressure is 16 bars. Additionally, we consider that the gas undergoes reversible adiabatic expansion (isentropic $\Delta S=0$) so that its outlet temperature (25°C) never approaches a value close to that of hydrate or condensate

formation.

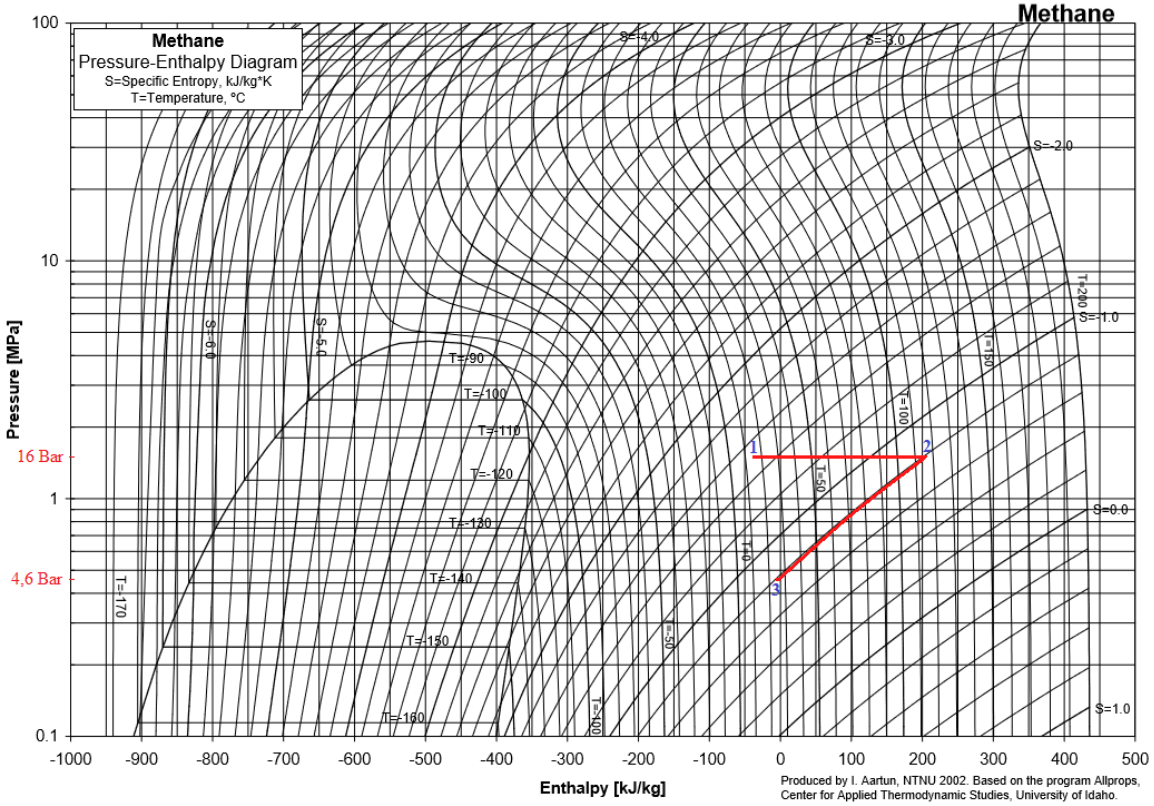

Figure 13. Moullier diagram for methane. [12]

The evolution of the open cycle of natural gas is shown in the P-H diagram for R50, as it is more than 85% methane. From this diagram, we can see graphically the characteristics of the points expressing the gas state for each stage of the cycle. The table below gives a clear idea of these characteristics for reversible and irreversible expansion.

Table 8. Natural gas characteristics for each stage in the system.

Points	Enthalpy [kJ/kg]	Entropy [kJ/kg °K]	Temperature [°C]	Pressure [bar]
1	-20	-1.45	15	16
2	200	-0.9	117	16
3	0	-0.8	25	4.6

4.4.1 Turbine performance

The next step is to design an exchanger capable of heating the incoming gas at high pressure through a turbine with an isentropic efficiency of 82%. **[12]**

$$\tau = \frac{16}{4.6} \quad (49)$$

$$\eta_{is} = 1 - 0.05\,\tau \quad = 82\% \qquad (50)$$

Where τ is the turbine's upstream-downstream pressure ratio.

4.4.2 Calculating power supplies

Returning to the table, we will select the data required to calculate the power supplied by the turbine and the preheater:

$$P_{Turbine} = \dot{m}\Delta H_{(2-3)} = 1860\ kW \quad = 1.86\ MW \qquad (51)$$

$$P_{Boiler} = \dot{m}\Delta H_{(2-1)} = \dot{m}c_p\Delta T_{(2-1)} = 2043\ kW \ = 2.04\ MW \qquad (52)$$

4.5 Preheater equipment selection

4.5.1 Thermal analysis

The most commonly encountered heat exchangers in gas preheating are straight tube and U-tube heat exchangers. They are distinguished primarily by the type of heat exchange surface between the two fluids, which dictates their respective behaviors. (see Appendix 4)

Table 9. Characteristic table of two fluids [13]

	Natural gas	**Water steam**
Cp [J/kgK]	2117	1850
Density [kg/Nm^3]	0.836	4.85
Reheater inlet temperature [°C]	15	180
Reheater outlet temperature [°C]	117	90
Flow [kg/h]	33440	658
Pressure[bar]	15-20	8

The desired power of the preheater is 2043 kW. To maintain this output, superheated water up to 180°C must be delivered at 5.3 kg/s, or a quantity of superheated steam must be withdrawn by the steam transformers. To ensure proper operation of stage B boilers, the steam return temperature must be half or higher than the temperature tapped. The auxiliary steam circuit is designed to supply steam to the heavy fuel oil or natural gas reheating circuit, in order to avoid the risk of fuel leaking into the steam lines if steam from the boiler is used (Figure 14).

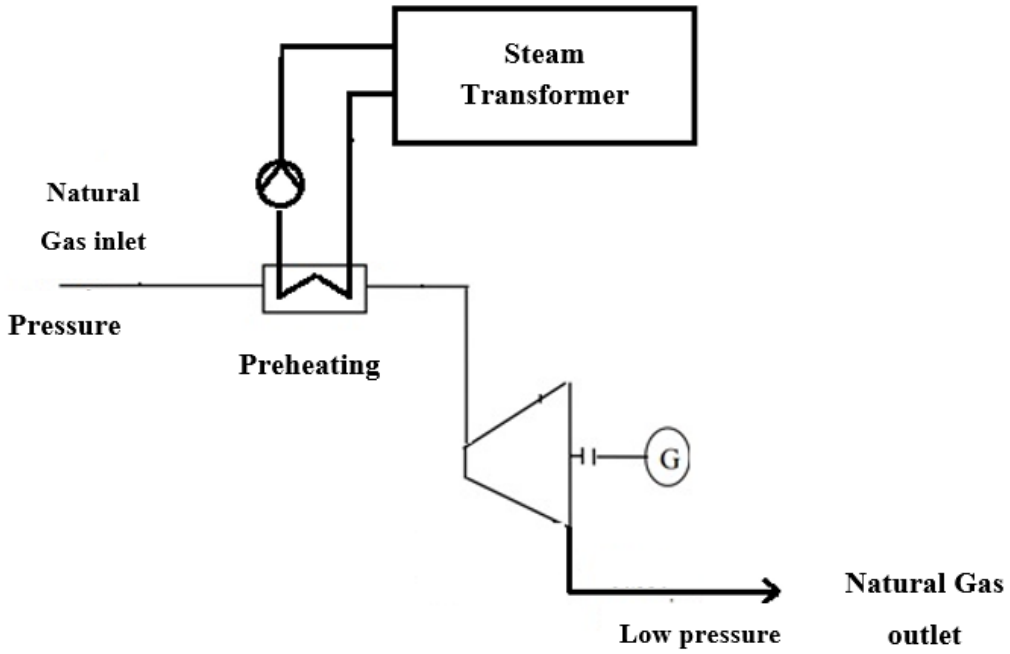

Figure 14. Preheater feed by Steam Transformer.

The steam transformer is a U-type heat exchanger designed to perform heat exchange between the body-side fluid (steam transformer feed water) and the tube-side fluid (steam from the auxiliary barrel). The assembled tube bundle is fastened to a tube sheet and supported by support plates arranged in appropriate spacing. (see Appendix 5).

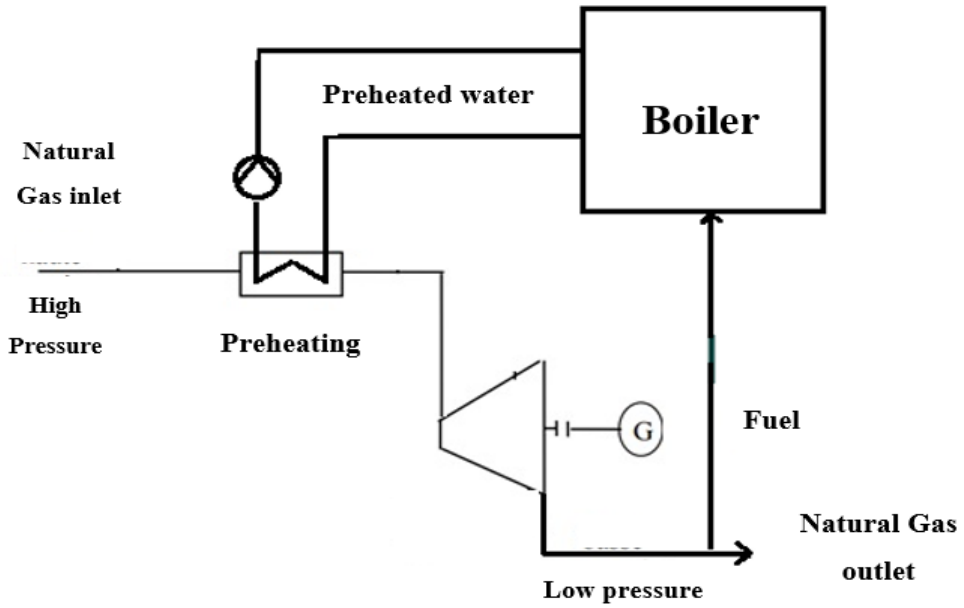

Figure 15. Preheater supply from a boiler.

Recovering energy lost at the gas expansion station can be of great benefit if a free source of preheating is used. In our case, however, the constraint is the steam transformer. In other words, its structure is not capable of ensuring proper system operation after the modification required for our needs, as it is inevitable to unbalance the auxiliary power supply. This led to the installation of an 80% efficiency gas-fired boiler capable of generating the necessary thermal power through a heat-transfer fluid. (Figure 15)

4.5.2 Choice of co-generator (gas engine)

In order to reduce the overall cost of the installation, we decided to use the heat from the flue gases of a generator already installed at the CPR to power our preheater. It therefore seems very interesting and even necessary to use this cogenerator.

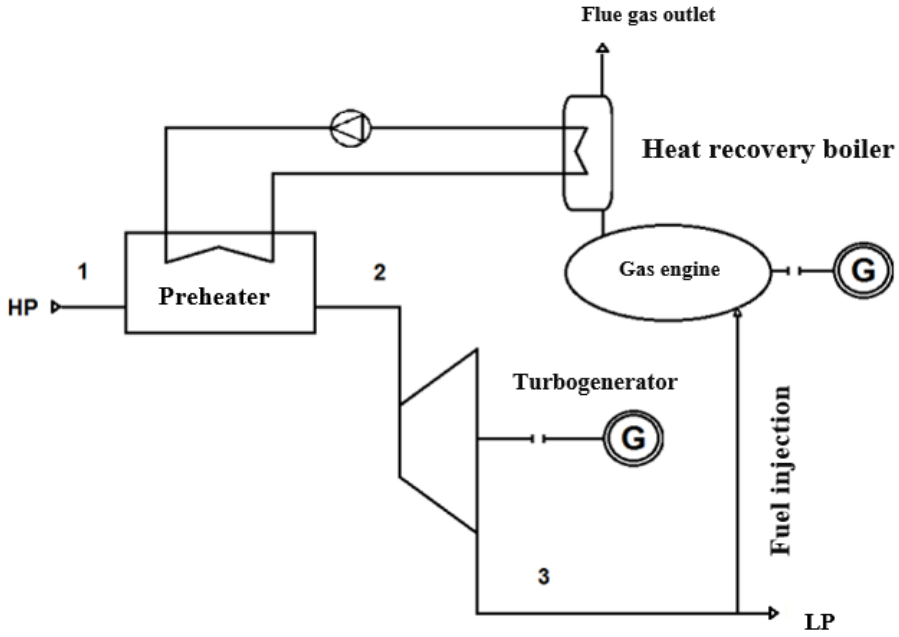

Figure 16. Preheater supply from a cogenerator.

The purpose of the cogenerator is to transform the fuel (natural gas) into mechanical energy, which is further transformed into electrical energy by the generator, and thermal energy, more than 70% of which is recovered in the heat. Our aim is to install a heat exchanger to recover this heat from the flue gas, so that its temperature reaches 500°C. A small proportion of the thermal energy is not recoverable: this is the heat released by radiation, engine convection and residual heat in the exhaust (110°C). The cogeneration engine studied in this tool is a conventional internal combustion engine, coupled to an alternator producing electricity.

Gas is generally preferred to fuel oil, and the gas supply is guaranteed because the gas engine can be supplied by a peak load taken from the gas circuit. The first advantage of gas is that its emissions are lower than those of fuel oil: an engine dedicated exclusively to peak-shaving only operates during peak hours, i.e., 4 hours a day for 4 months a year. This is usually an oil-fired unit. In contrast, cogeneration will operate as continuously as possible. This is usually a gas-fired unit. Another advantage is that gas engines are generally more efficient, but at a higher investment cost.

4.5.3 Estimation of exhaust gas properties

The heat contained in the exhaust is generally recovered by a fume-water exchange in a cross-current exchanger. Exhaust temperatures and flow rates also depend on the engine selected. The expression for exchanged flow is therefore written as follows:

$$\phi = (\dot{m} c_p \Delta T)_h = (\dot{m} c_p \Delta T)_c \quad (53)$$

As already mentioned in the previous paragraph, the power of the heater to be recovered is 2.043 MW. To ensure optimum transfer of the heat released by the engine at 500°C, it is necessary to set the flue gas characteristics. To do this, the flue gas outlet temperature can be estimated by a constraint that will be used as a solution for determining ΔT. This constraint is the dew point temperature of sulfuric acid.

* Formation of H_2SO_4

Temperature, oxygen content and humidity, leading to the formation of sulfuric acid, which is responsible for corrosion. Operating difficulties caused by fouling and corrosion at high and low temperatures are due to the formation of SO_3 from the sulfur contained in the fuel. Under certain conditions of metal skin temperature and hygrometry, SO_3 condenses to form sulfuric acid H_2SO_4

- Combustion of S gives:

$$S + O_2 \rightarrow SO_2$$

- The presence of excess air then gives the following equilibrium:

$$SO_2 + 1/2\ O_2 \rightarrow SO_3$$

- And with the presence of water, we obtain:

$$H_2O + SO_3 \rightarrow H_2SO_4$$

The dew point of the flue gas varies according to the percentage of SO_3 contained in the flue gas The "water-acid" mixture condenses on the cold parts as soon as the temperature reaches the sulfuric acid dew point. This temperature can reach values below $100\,℃$ **[13].** The required outlet temperature is therefore $110\,℃$.

$$\Delta T = T_{in} - T_{out} = 500 - 110 = 390°C \qquad (54)$$

The gas released into the atmosphere consists essentially of:N_2, CO_2 and H_2O, Other gases with low contents such as *CO*, NO_X and SO_2 have no influence on the approximate value of the total heat capacity of the smoke to be determined, in order to know the flow rate sufficient for preheating.

4.5.3.1 The natural gas combustion reaction

The composition of the natural gas supplied to the engine's displacements is shown in the following table:

Table 10. Composition of the natural gas fed to the combustion chamber. (Appendix 7)

Component	Formula	Molar mass (g/mol)	Molar fraction (%)
Methane	CH_4	16	85
Ethane	C_2H_6	30	8.85
Propane	C_3H_8	44	1.47
Butane	C_4H_{10}	58	0,22
Pentane	C_5H_{12}	72	0.23
Nitrogen	N_2	38	2.9
Carbon dioxide	CO_2	44	1.14
Sulfur dioxide	SO_2	64.06	0.1
Water	H_2O	18.01	0.09

Nitrogen remains neutral during the combustion reaction, so the hydrocarbons will react with the air to produce smoke at the engine's displacement output.

The general stoichiometric equation for combustion in air is:

$$C_xH_yO_zN_uS_v + \left(x + v + \left(\frac{y}{4}\right) - \left(\frac{z}{2}\right)\right)(O_2 + 3{,}77N_2) \rightarrow xCO_2 + vSO_2 + \left(\frac{y}{2}\right)H_2O + \left(\left(\frac{u}{2}\right) + 3{,}77\left(x + v + \left(\frac{y}{4}\right) - \left(\frac{z}{2}\right)\right)\right)N_2 \qquad (55)$$

The fictitious formula C_xH_y for natural gas is determined:

$x = \sum$ number of carbon atoms in component × fraction of component in mixture

$y = \sum$ number of hydrogen atoms in the component × fraction of the component in the mixture

$$x = [(85 \times 1) + (8.85 \times 2) + (1.47 \times 3) + (0.22 \times 4) + (0.23 \times 5)]/100 \qquad (56)$$

$$y = [(85 \times 4) + (8.85 \times 6) + (1.47 \times 8) + (0.22 \times 10) + (0.23 \times 12)]/100 \quad (57)$$

$$\boldsymbol{x = 1.0914} \qquad \textit{and} \qquad \boldsymbol{y = 4.0982}$$

The fictitious formula for natural gas is therefore: $\boldsymbol{C_{1,0914}H_{4,0982}}$

In the reaction the product obtained at the outlet is formed solely of carbon dioxide CO_2, water H_2O and nitrogen N_2 represented by the following reaction:

$$C_xH_y + \left(x + \left(\frac{y}{4}\right)\right)(O_2 + 3{,}77N_2) \rightarrow \quad xCO_2 + \left(\frac{y}{2}\right)H_2O + 3{,}77\left(x + \left(\frac{y}{4}\right)\right)N_2 \quad (58)$$

In our case, this gives:

$$C_{1,0914}H_{4,0982} + 2.116\ (O_2 + 3{,}77\ N_2) \rightarrow \quad 1.0914\ CO_2 + 2.049\ H_2O + 7.977\ N_2 \quad (59)$$

Table 11. Fume composition in mass and molar fractions

Element	N_i (mole)	x_i	M_i(g/mole)	W_i	Cp (J/Kg)
CO_2	1.0914	0.0981	44.01	0.155	1.076
H_2O	2.049	0.1843	18.015	0.119	2.121
N_2	7.977	0.7175	28.013	0.724	1.101

$With:\ N_t = \sum N_i = \boldsymbol{11.117}\ mole\ ;\ M_t = \sum N_i \times M_i = \boldsymbol{308.405}g\ ;\ X_i = N_i/N_t$

And $W_i = N_i \times M_i/M_t$

4.5.3.2 Calculation of flue gas heat capacity

The table below gives the values of the heat capacity at constant pressure from 273 to 1500 Kaccording to this formula: **[13]**

$$Cp = a + bT + cT^2\ (J.mol^{-1}\,K^{-1}). \quad (60)$$

Table 12. Molar heat capacities at constant pressure Cp ($\boldsymbol{J.mol}$-1 $\boldsymbol{K}$-1) for different temperatures. [13]

Gas	Coefficients			Cp values at selected temperatures in K							
	A	$b.10^{-3}$	$c.10^{-6}$	**273**	**373**	**473**	**673**	**873**	**1073**	**1273**	**1473**
H_2	29.3	-0.84	2.09	29.23	29.28	29.37	29.68	30.16	30.8	31.62	32.6
O_2	25.73	12.97	-3.77	28.99	30.04	31.02	32.75	34.18	35.31	36.13	36.65
Cl_2	36.83	0.84	0	37.06	37.14	37.23	37.4	37.56	37.73	37.9	38.07
Br_2	35.15	4.19	-1.26	36.2	36.54	36.85	37.4	37.85	38.2	38.44	38.59
N_2	27.62	4.19	0	28.76	29.18	29.6	30.44	31.28	32.12	32.95	33.79

CO	27.62	5.02	0	28.99	29.49	29.99	31	32	33.01	34.01	35.01
CO_2	32.22	22.18	-3.35	38.03	40.03	41.96	45.63	49.03	52.16	55.03	57.62
CH_4	14.23	75.3	-18	33.45	39.81	45.82	56.75	66.25	74.3	80.92	86.09
HCI	28.04	1.67	-1.67	28.37	28.43	28.46	28.41	28.23	27.91	27.46	26.88
H Br	25.53	4.19	-0.84	26.61	26.98	27.32	27.97	28.55	29.06	29.5	29.88
H_2O	30.13	10.46	0	32.99	34.03	35.08	37.17	39.26	41.35	43.45	45.54
NH_3	31.81	15.48	5.86	36.47	38.4	40.44	44.88	49.79	55.17	61.01	67.33

Table 13. Molar heat capacity at constant volume Cv ($J.mol$-1 K-1) for different temperatures. [13]

Gas	**Temperature (K)**				
	173	**273**	**373**	**673**	**873**
He, Ne, Ar	12.47	12.47	12.47	12.47	12.47
H_2	17.49	20.59	20.8	20.88	20.93
N_2	20.72	20.72	20.76	22.18	22.68
O_2	20.84	20.93	21.55	24.48	25.91
Cl_2		24.48	24.61	26.11	26.78
H_2O			26.66	28.54	31.81
CO_2		28.25	32.98	41.26	45.62

According to the table Cp at $500\,℃$=$773\,°K$ is calculated as follows

$For\ CO_2$:

$$Cp(773°K) = 32.22 + (22.18.10^{-3} \times 773) - (3.35.10^{-6} \times 773^2)$$

$$= 47.36\,J/mol\,K \qquad (61)$$

$$\boxed{\boldsymbol{Cp_{CO_2} = 1.076\,J/gK}}$$

$For\ H_2O$:

$$Cp = 30.13 + (10.46.10^{-3} \times 773) = 38.05\,\frac{J}{molK} \qquad (62)$$

$$= \frac{38.21}{18.01} = \ \boldsymbol{2.121\,J/gK}$$

$For\ N_2$:

$$Cp = 27.62 + (4.19.10^{-3} \times 773) = 30\,\frac{03J}{molK} \qquad (63)$$

$$= \frac{30.858}{28.013} = \mathbf{1.101 J/gK}$$

Cp of the mix can be calculated by $Cp = \sum W_i \times Cp_i$

$$Cp = (1.076 \times 0.155) + (2.121 \times 0.119) + (1.101 \times 0.724) = \boxed{\mathbf{1.216\, J/gK}} \quad (64)$$

* Reaction with 60% excess air **[13]**

In our case. this gives:

$$\frac{1}{R} = 1 + e = 1.6 \qquad (65)$$

Where R is richness; e is excess air

$$C_{1.0914}H_{4.0982} + 1.6 \times 2.116\,(O_2 + 3.77\,N_2) \rightarrow \quad 1.0914\,CO_2 + 2.049\,H_2O$$
$$+1.6 \times 7.977\,N_2 + 0.6 \times \left(1.0914 + \left(\frac{4.0982}{4}\right)\right) O_2 \quad (66)$$

Table 14. Composition of flue gases with excess air in mass and molar fractions

Element	N_i (mole)	x_i	M_i(g/mole)	W_i	Cp (KJ/Kg)
CO_2	1.0914	0.0635	44.01	0.1038	1.076
H_2O	2.049	0.1193	18.015	0.0797	2.121
N_2	12.76	0.7432	28.013	0.7725	1.101
O_2	1.269	0.0739	16	0.0438	2.09

With: $N_t = \sum N_i = 17.169\ mole$; $M_t = \sum N_i \times M_i = 462.695\ g$; $Xi = Ni/N_t$

Et $W_i = N_i \times M_i/M_t$

According to the table Cp of O_2 at 500 $°C$ is calculated as follows:

$$Cp = 25.73 + (12.97.10^{-3} \times 773) - (3.77.10^{-6} \times 773^2) = 33.503\ J/molK \quad (67)$$

$$\boxed{\mathbf{Cp = 2.09 \quad J/gK}}$$

Finally, Cp of the mixture can be calculated by $Cp = \sum W_i \times Cp_i$

$$Cp = (1.076 \times 0.1038) + (2.121 \times 0.0797) + (1.101 \times 0.7725) + (2.09 \times 0.0438)$$

$$\boxed{\mathbf{Cp_f = 1.223\ kJ/kgK}} \qquad (68)$$

4.5.3.3 Fume flow

Once we know the heat capacity of the gases released in the exhaust of a gas engine and the energy that can be recovered through the fumes, we can deduce its flow rate using this formula:

$$\dot{m}_f = \frac{P}{Cp.\Delta T} = \frac{2043}{1.223\times(500-110)} = 4.28 kg/s \qquad (69)$$

With:

P: Recovered power (W).

$\dot{m}$: Off-gas flow (kg/s).

ΔT : The temperature difference between the inlet and outlet of the recovery exchanger (on the flue gas side). ($℃$)

The fume output is therefore $\boldsymbol{\dot{q}_m = 4,28\ kg/s}$

4.6 Sizing the flue gas/water heat exchanger

Our gas engine produces fumes at 500 $℃$ which are used to preheat water from 90 to 180 $℃$. This generator produces 12600 kg of fumes per hour. Considering that the combustion of one kilogram of gas requires 48 kg of air.

The unit to be sized is a cross-flow tubular exchanger with two passes on the tube side. These are exchangers in which the flow around the tubes is substantially perpendicular to the tube bundle. This arrangement is used for exchanges between gas circulating in the shell and liquid circulating in the tubes. **[14]**

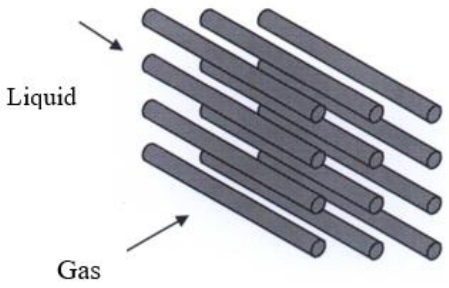

Figure 17. Flow perpendicular to the tube bundle.

Water flows vertically through the tubes. and flue gas flows horizontally around them. The wall temperature T_p of the tubes must be above 110°C to avoid corrosion due to condensation of sulfur compounds.

4.6.1 Beam geometry

The beam can be in line (figure 19) or staggered (figure 18). **[14]**

The bundle is staggered if the tubes are placed at the vertices of isosceles triangles: the pitch is then said to be triangular (with the special case of equilateral triangular pitch).

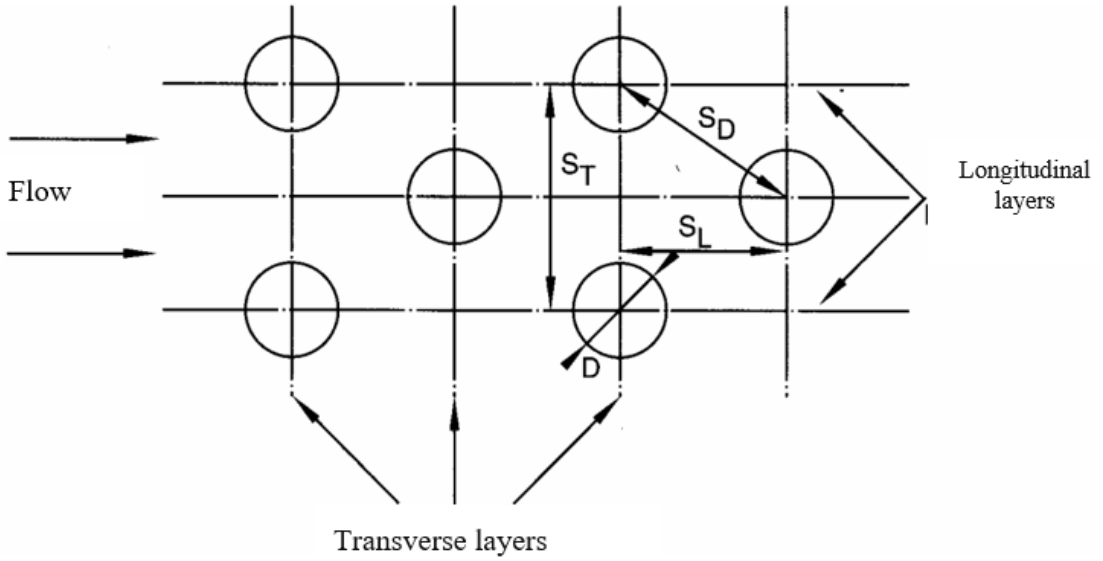

Figure 18. Staggered beam.

In an in-line beam. the tubes are arranged at a rectangular pitch. which may in particular be a square pitch.

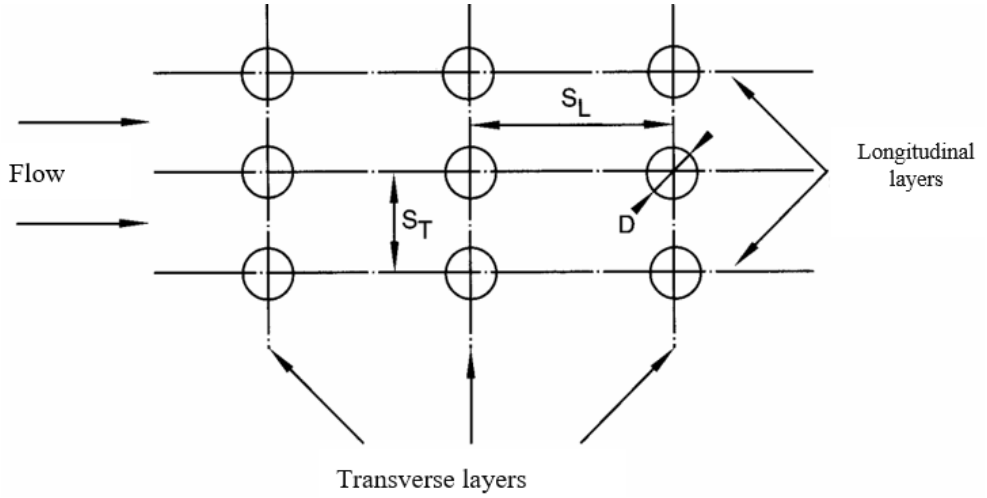

Figure 19. In-line beam.

The quantities representative of beam geometry is listed below:

D: external tube diameter (mm)

S_L : longitudinal pitch (center-to-center distance in direction of flow) (mm)

S_T : transverse pitch (axes perpendicular to the flow) (mm)

S_D: diagonal pitch (for a staggered beam)

Adimensioned (or relative) steps

$$e_L^+ = \frac{S_L}{D} \ ; \ e_T^+ = \frac{S_T}{D} \ ; \ e_D^+ = \frac{S_D}{D} \qquad (70)$$

L : Beam length (mm)

N_L : Number of longitudinal layers (rows of tubes parallel to the flow)

N_T : Number of transverse layers (rows of tubes perpendicular to the flow).

‹ The number of tubes in a transverse web is therefore equal to the number NL of longitudinal webs.

In a staggered beam ST is twice the distance between two longitudinal webs.

The notation S_L, S_T, S_D is common but not very happy: these quantities are not cross-sections but lengths; thus. the cross-sectional area between two tubes is $(S_L - D)L$.

The choice of geometry may of course depend on manufacturing constraints. From a thermal point of view the staggered bundle ensures a higher transfer coefficient (approximately 10% higher than the in-line bundle) due to better fluid mixing with a slightly more uniform temperature distribution at the periphery of each tube than in the in-line bundle. On the other hand, pressure losses are higher. with the aim of minimizing pressure losses in the hydraulic flue gas flow. We need to model our exchanger with tubes forming an in-line bundle with square pitch and relative pitch:

$$e^+ = e_T^+ = e_L^+ = 1.4 \qquad (71)$$

They have an outer diameter of 40millimeters and an inner diameter of 35millimeters. For each flow the Reynolds number is fixed at $Re_c = 40\ 000$ in the tubes (cold fluid) and $Re_h = 7000$**[14]** in the calendar (hot fluid. reference velocity = flow velocity in empty calendar).

4.6.2 Calculating the dynamic viscosity and thermal conductivity of smoke

For the temperature range under consideration the average flue gas characteristics are:

Table 15. Fume characteristics at Tm =305°C and atmospheric pressure.

Element	Wi	μ(kg/ms)	λ(W/mK)	Cp(kJ/Kg)
CO_2	0.1038	$2.67.10^{-3}$	0.015	1.076
H_2O	0.0797	$2.0.10^{-3}$	0.54	2.121
N_2	0.7725	$2.837.10^{-3}$	0.045	1.101
O_2	0.0438	$3.338.10^{-3}$	0.048	2.09

With $\lambda_{fume} = \sum \lambda i \times wi = 0.081 W/m.K$ and $\mu_{fume} = \sum \mu i \times wi = 2.77.\ 10{-}5 kg/m.$

And Cp=1223 J/kgK; ρ_{fume}=1.188 kg/m^3 ; ρ_{Water}=928.3 kg/m^3 ; μ_{Water}=0.198.10-3 kg/m.s ; Cp_{Water}=4283 J/kgK ; λ_{Water} =0.684 W/m K (see Appendices 10 and 11).

4.6.3 Wall temperature profile

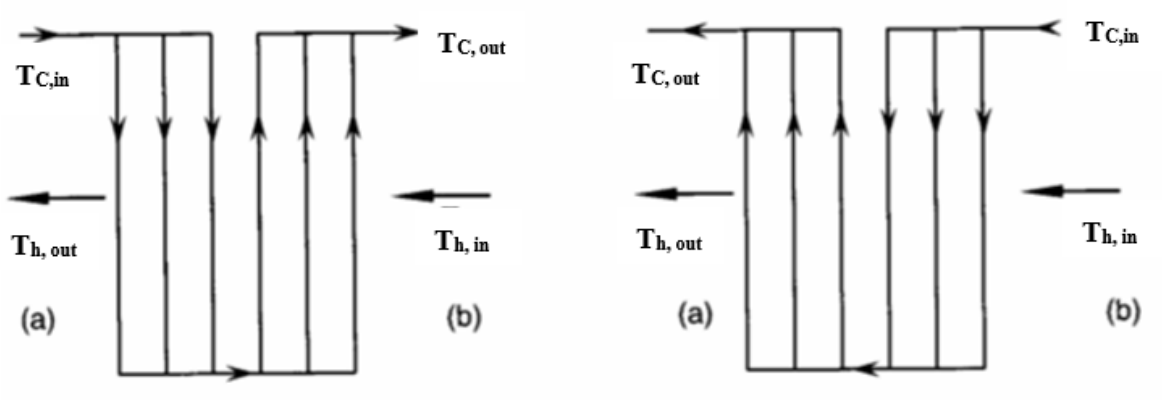

Figure 20. Tubular cross-current exchanger Left: opposite inlets. Right: inlets on the same side.

The first step is to calculate the unit heat flow rates.

-For the cold fluid (water) the mass flow rate is 4.3 kg/s. Its heat density depends slightly on temperature. It is rounded off to Cp=$4283 J/kgK$: **[15]**

$$q_{tc} = q_{mc} Cp_c = 5.3 \times 4283 = 22.7.10^3 W/K \qquad (72)$$

For hot fluid (fume)

$$q_{t.h} = 4.3 \times 1223 = 5.23.10^3 W/K \qquad (73)$$

In passing we note that:

$$q_{tmin} = q_{tc} = 5.23.10^3 W/K \qquad (74)$$

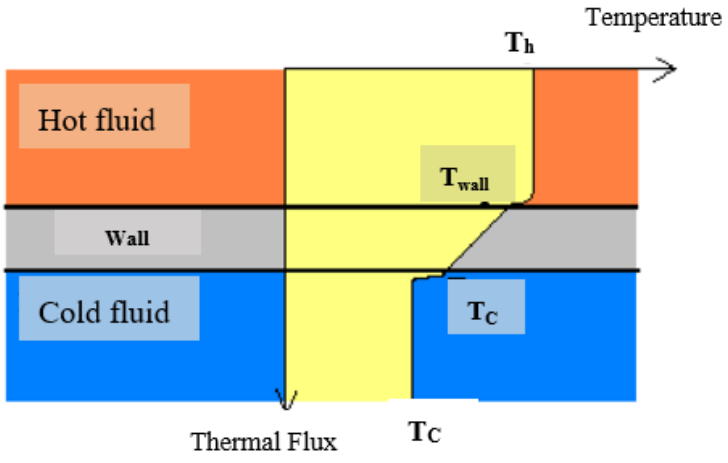

Figure 21. Temperature profile during exchange through a surface element dS. [21]

As a first approximation the local wall temperature is:

$$Tp \approx (T_{Water} + T_{fume})/2 \qquad (78)$$

With opposite inputs Figure 20, we have:

* For (a): Water at 90 °C; fume at 110 °C. is:

$$Tpa \cong \frac{90 + 110}{2} = 100°C < 110°C \qquad (79) \qquad "Risk\ of\ condensation"$$

* For (b): Water 180 °C; fume at 500 °C. is:

$$Tpb \cong \frac{500 + 180}{2} = 340°C \qquad (80) \qquad "No\ problem"$$

This solution should be avoided: there is a high risk of condensation towards the flue outlet.

With inputs on the same side:

* For (a): Water at 180 °C; smoke at 110 °C. therefore:

$$Tpa \cong \frac{110 + 180}{2} = 145°C > 110°C \qquad (81) \quad "Alright"$$

* For (b): Water at 90 °C; smoke at 500 °C:

$$Tpb \cong \frac{500 + 90}{2} = 295°C > 110°C \qquad (82) \quad "Still\ good"$$

Conclusion: It's best to place the tube inlets on the same side of the exchanger.

4.6.4 Reference values

The conventional reference length of the flow in the bundle is the outside diameter of the tubes: L° = D **[14]** as reference velocity V°, we adopt the frontal flow velocity in the empty calendar, the tubes being assumed to be removed; calling S° the cross-sectional area of the calendar:

$$V^0 = \frac{q_m}{\rho S^0} = \frac{q}{S^0} \qquad (83)$$

In particular. here we have:

$$Re = \frac{V^0 D}{\upsilon} = \frac{q_m D}{\mu S^0} \qquad (84) \qquad and \qquad St = \frac{h}{\rho Cp V^0} = \frac{h S^0}{q_m Cp} \qquad (85)$$

Where:

Re represents the Reynold number

St Represents the Stanton Number

The reference velocity V_c^0 on the cold fluid side refers to the flow of water through the tubes.

$$Re_c = \frac{V_c^0\, d}{\upsilon_c} = 40000 \qquad (86)$$

V_c Must be evaluated at the average mixing temperature of the water:

$$T_{m.water} \cong \frac{90 + 180}{2} = 135°C \quad (87) \quad with \quad \upsilon_f = \frac{\mu_c}{\rho_c} = 0.213.\frac{10^{-6}m^2}{s} \qquad (88)$$

We deduce:

$$V_c^0 = \frac{40000 \times 0.198.\,10^{-3}}{928.3 \times 35.\,10^{-3}} = 0.24\ m/s \qquad (89)$$

Reference velocity V_h^0 on the hot fluid side Now we turn to the flue gases. knowing that:

$$Re_h \frac{V_h^0\, D}{\upsilon_h} = 7000 \quad (90) \qquad with \quad \upsilon_h = \frac{\mu_h}{\rho_h} = \frac{2.77.\,10^{-5}}{1.188} = 2.33.10^{-5}m^2/s \quad (91)$$

From this. we derive:

$$V_h^0 = \frac{Re_h \upsilon_h}{D} = \frac{7000 \times 2.33.\,10^{-5}}{40.\,10^{-3}} = 4.07\ m/s \quad (92)$$

4.6.5 Calculation of the average exchange coefficient

It is still necessary to know the overall exchange coefficient defined by the equation:

$$d\phi = k(T_h - T_c)dS \qquad (93)$$

Heat transfer from the hot fluid to the cold fluid is the result of three successive phenomena:

- ✓ Convection between the hot fluid and the outer face of the solid wall.
- ✓ Conduction through this solid wall.
- ✓ Convection between the inside of the solid wall and the cold fluid.

Convection in the hot fluid is governed by a convection coefficient h_h which defines the convective thermal resistance $1/h_hS$.

Convection in the cold fluid is governed by a convection coefficient h_c which defines the convective thermal resistance $1/h_cS$.

Conduction through the solid wall of thickness e and thermal conductivity λ is accounted for by a conduction thermal resistance $e/\lambda S$ so that the heat flow transferred from the hot fluid to the cold fluid is given by the expression:

$$k = \frac{1}{\frac{1}{h_h} + \frac{e}{\lambda} + \frac{1}{h_h}} \qquad (94)$$

This modelling still needs to be completed on two points to correctly account for the phenomena in our real exchanger:

In the above relation, we assumed the same exchange surface area S on the hot and cold sides. In our case, the exchange surface does not have the same extent in contact with the two fluids. We must therefore introduce exchange surfaces S_h and S_c and relate the overall exchange coefficient. either to the unit of exchange surface on the hot side and note it k_h, or the unit of heat exchange surface on the cold side and is noted k_c.

In addition, after a certain period of operation the heat exchanger walls become covered with a film of dirt. These deposits of scale and dirt have a low thermal conductivity compared with that of metal, and therefore, constitute additional thermal resistances $R_{eh}\ and\ R_{ec}$ opposing exchange.

Ultimately, the actual performance of the heat exchanger will be deduced from the calculation of either of the following two overall exchange coefficients: **[14]**

$$k_h = \frac{1}{\frac{1}{h_h} + R_{ec} + \frac{e}{\lambda_{steel}}\frac{\Sigma_h}{\Sigma_m} + \left(R_{ec} + \frac{1}{h_c}\right)\frac{\Sigma_h}{\Sigma_c}} \qquad (95)$$

$$k_c = \frac{1}{\frac{1}{h_c} + R_{ec} + \frac{e}{\lambda_{steel}}\frac{\Sigma_c}{\Sigma_m} + \left(R_{eh} + \frac{1}{h_h}\right)\frac{\Sigma_c}{\Sigma_h}} \qquad (96)$$

With:

S_c: is the exchange surface area on the cold side in (m^2).

S_h: is the area of the hot-side exchange surface in (m^2).

S_m: is the area of the average exchange surface in (m^2).

$R_{eh}\ and\ R_{ec}$: are the resistances per unit area of the fouling films deposited on the hot and cold sides of the exchange surface in $(m^{2\circ}C/W)$.

$k_h\ et\ k_c$: Are expressed in $(W/m^{2\circ}C)$.

The Stanton number (St) is a dimensionless number used in heat and mass transfer operations. It represents the ratio between total transfer and convective transfer. It is defined as follow:

$$St = \frac{h}{v\ \rho\ Cp} \qquad (97)$$

With

h: Heat transfer coefficient in $(\mathrm{W/m^2k})$

v: speed in (m/s)
P : Mass density in (kg/m^3)
C_p: calorific capacity in (J/kg.K)

Or also:**[14]**

$$St = 0.023\left\{1 + 6.2\left(\frac{e_T^+ + 0.90}{e_T^+ - 0.98}\right)^{0.6}(e_L^+)^{-0.2}\right\}Re^{-0.32}Pr^{\alpha} \qquad (98)$$

$With: Pr\ the$ Prandtl number > 0.66 ; $10^2 < Re < 2.10^5$; $N_T \geq 10$

Cooling fluid: $\alpha = -0.6$; Hot Fluid: $\alpha = -0.7$

$St, Re\ and\ Pr$ at average mixing temperature T_m

To calculate St, then h, we will use the following formulas (Boissier), based on the conventional quantities we've just defined and in particular the reference velocity V^0. They are valid over a wide range of Reynolds numbers since the sinusitis in the fluid's path generate stirring that resembles turbulent motion even at low Reynolds values. The laminar-turbulent distinction is therefore irrelevant.

4.6.5.1 Heat transfer coefficient h warm side (in shell)

The Reynolds number is given by the constructor $Re_h = 7000$ with a reference speed in the empty calendar of $4.07\ m/s$. compatible with the formulas. The beam is in line so, it follows that:$e_T^+ = e_L^+ = e^+$=1.4. Assuming that the number of sheets is at least 10 the Stanton number is taken from formula below with α=-0.7 for the hot fluid. The Prandtl number is calculated at temperature $T_{m.h}$. giving:

$$Pr_h = \frac{\mu Cp}{\lambda} = \frac{2.77.10^{-5} \times 1223}{0.081} = 0.418 \qquad (99)$$

The result is :

$$St = 0.023.\left\{1 + 6.2.\left(\frac{1.4 + 0.90}{1.4 - 0.98}\right)^{0.6}.1.4^{-0.2}\right\}.7000^{-0.32}.0.418^{-0.7} \qquad (100)$$

$$St = 0.0425$$

The exchange coefficient h_h can be deduced from St :

$$h_h = St_h \rho_h Cp_h V_h^0 = 0.042 \times 1.188 \times 1223 \times 4.07 \qquad (101)$$

$$\boxed{h_h = 248\ W/m^2K}$$

4.6.5.2 Coefficient of exchange h_c on cold fluid side (in tubes)

We know that $Re_c = 40\,000$ in the absence of information on wall roughness, it's reasonable to assume that we're in a "smooth turbulent" regime. We will therefore use the formula of Dittus and Boelter with: α=-0.6 (cold fluid) provided that we have L/d>60. which will have to be verified at the end of the calculation:

$$St_c = 0.023\ Re_c^{-0.2} Pr_c^{-0.6} = 0.023\ \times 40000^{-0.2} \times 1.239^{-0.6} = 0.00243 \quad (102)$$

For water at $T_{m.c} = 135°C\ \ et\ \ Pr_c = 1.24$

From this we deduce $h_c = St_c \rho_c Cp_c V_c^0 = 0.00243 \times 928.3 \times 4283 \times 0.24$ (103)

At temperature $T_{m.c} = 135°C$ the tables give for water: ρ=928.3 kg/m3

And $C_{p.c}$=4283 J/kgK thus:

$$h_c = 2318.7\ W/m^2K$$

4.6.5.3 Pipe dimensions

The overall coefficient k_h hot fluid side is then calculated using:

$$k_h = \frac{1}{\frac{1}{h_{.h}} + R_{e.h} + \frac{e}{\lambda_{steel}}\frac{\Sigma_c}{\Sigma_m} + \left(R_{e.c} + \frac{1}{h_c}\right)\frac{\Sigma_h}{\Sigma_c}}$$

$$= \frac{1}{\frac{1}{248} + 20.10^{-4} + \frac{5.10^{-3}}{19.46}\frac{40}{37.5} + \left(4.10^{-4} + \frac{1}{2318.7}\right)\frac{40}{35}} \quad (104)$$

The choice of tube material is important from the point of view of corrosion. We have therefore chosen stainless steel whose thermal conductivity is estimated at an average wall temperature $T_m = 305°C$ by the following formula (see Appendix 6).

$$\lambda_{steel} = 0.0162\ T(°C) + 14.52 = 19.46\ W/m\ K \quad (105)$$

The ratio of exchange surfaces is equal to the ratio of diameters.

$$\frac{\Sigma_h}{\Sigma_m} = \frac{2\pi L\ R}{2\pi Lr} = \frac{D}{d} \quad (106)$$

After a certain period of operation the heat exchanger walls become covered with a film of impurities. These deposits of scale and dirt have a low thermal conductivity compared with that of the metal (steel). and therefore, constitute additional thermal resistances R_{eh} and R_{ec} opposed to exchange. Comparative measurements between commissioning conditions then operation over time have enabled us to deduce some fouling resistance values (see Appendix 1).

We get: $k_h = 137.8\ W/m^2\ K$

The efficiency of this exchanger is:

$$\varepsilon = \frac{\phi}{q_{t\,min}(T_{h.in} - T_{c.in})} = \frac{2043}{4.2805 \times (500 - 90)} = 0.95 \qquad (107)$$

The heat exchanger is a cross-flow, single-fluid heat exchanger, with a single pass over the mixed fluid. The minimum heat flow rate is that of the flue gas that is of the mixed fluid in this case (see Appendix 8) gives:

$$NUT = -Ln\left[1 + \frac{1}{Z}\ln\left(1 - \varepsilon Z\right)\right] \qquad (108)$$

$$With \qquad Z = \frac{q_{tmin}}{q_{tmax}} = \frac{4280.5}{18416.9} = 0.232 \qquad (109)$$

And finally, $NUT = -Ln\left[1 + \frac{1}{0.232} \times \mathrm{Ln}(1 - 0.95 \times 0.232)\right] = 0.272$ (110)

From NUT we deduce the value of the heat transfer surface Σ_h on the hot fluid side:

$$NUT = \frac{k_h \Sigma_h}{q_{tmin}} \quad (111) \qquad thus \qquad \Sigma_h = \frac{0.272 \times 4280.5}{137.8} \qquad (112)$$

$$\Sigma_h = 10.33\ m^2$$

Tube bundles the heat exchange surface Σ_h on the hot fluid side corresponds to the outside diameter of the tubes: D= $40.10^{-3}m$. If L_t is the total length of the tubes. then:

$$\Sigma_h = \pi D L_t \quad (113) \ and \qquad L_t = \frac{8.45}{\pi \times 40.10^{-3}} = 82.24\ m \qquad (114)$$

Consider $\boldsymbol{n}$ as the number of tubes required in each pass to ensure the required flow rate and $\boldsymbol{S_t}$ as the total cross-sectional area of the tubes:

$$S_t = n\frac{\pi d^2}{4} \qquad (115)$$

To obtain n. $S_t$must first be calculated from the water flow expression

$$q_{mc} = \rho_c S_t V_c \qquad (116)$$

In a flow calculation, the density ρ_c must be evaluated at the average mixing temperature in this case T_{mc} which gives $\rho_c = 928.3\ kg/m^3$

Furthermore $V_c = V_c^0 = 0.24\ m/s$ and $q_{mc} = 4.3\ kg/s$ so

$$S_t = \frac{q_{mc}}{\rho_c V_c} = \frac{4.3}{928.3 \times 0.24} = 0.024\ m^2 \qquad (117)$$

$$n = \frac{4S_t}{\pi d^2} = \frac{4 \times 0.019}{\pi \times (35.10^{-3})^2} = 24.96 \qquad (118)$$

This means *25* tubes per pass. total ***N=50 tubes***. The length of each tube is given by:

$$L = \frac{L_t}{N} = \frac{67}{40} = 1.34\ m \qquad (119)$$

Verification: We now need to verify that the length of each tube satisfies the condition L/d > 60. However, this is not the case. as here we have L/d <60: S_{tc} must be multiplied by a factor. This will increase the overall heat transfer coefficient by a few percent and typically, we would have to iterate with this new value. However, we can skip repeating the calculations in this instance. As for h_c is concerned, given considering the total number of tubes, the condition "number of layers greater than 10" is realistic.

4.7. Sizing the gas/water heat exchanger

Upstream of the expansion turbine, a shell-and-tube heat exchanger is to be installed. designed to increase the natural gas flow of 33 440 kg/h from 15 to 110 $°C$. The primary fluid flowing through the tubes is superheated water arriving at 180 $°C$ and leaving at 90 $°C$. **[15]**. The tubes have an internal diameter of 20 *mm* and the flow velocity adopted is such that $Re = 20\ 000$. The overall exchange coefficient k is estimated at 450 W/m^2K.

4.7.1 Water mass flow calculation

The following thermo-physical characteristics are assumed for overheated water:

$Cp_{waterc} = 4283J/kgK$; ρ = 928.3 kg/m^3 and μ=0.198.10^{-3}*kg/m. s* (see Appendix 11).

First. let's calculate the unit heat rates. For natural gas, we generally assume Cp_{gas}= 2117 *J/kgK*. The thermal power is obtained from the gas values C_{gas}=19664.5 W/K

We now derive the overheated water flow rate from the balance sheet: $C_{water} = 22.7.10^3 W/K$

$$m_{water\,h} = \frac{2045}{4.283 \times (180 - 90)} = 5.3\ kg/s \qquad (120)$$

4.7.2 Calculating the exchange surface between water and natural gas

In the same way the exchange surface:

$$\Sigma = 10.33m^2$$

$$\Sigma_c = \pi D L_t \text{ and } L_t = \frac{10.33}{\pi \times 35.10^{-3}} = 93.99\ m \qquad (121)$$

4.7.3 Calculating heat exchanger dimensions

As a general rule Reynold's number represents the ratio between the inertial and viscous forces of a fluid flow. This dimensionless number appears naturally when dimensioning the Navier-Stokes equations. It depends on the pipe shape, and wall condition, for forced

convection in a turbulent pipe ($Re > 10\ 000$). By applying Reynold's formula we can deduce the water velocity in the tubes of our heat exchanger:

$$Re = 20\ 000 = \frac{\rho V D_h}{\mu} \qquad (122)$$

ρV is the mass velocity of the fluid in $kg/m^2 s$

$\rho V = \frac{\dot{m}}{s}$ with $\dot{m}$ mass flow in kg/s

S: cross-sectional area of the fluid stream in m^2

D_h is the hydraulic diameter in m: where D_h is equal to the pipe diameter D

$D_h = \frac{4s}{p}$ where s: cross-sectional area of the fluid stream in m^2

P: perimeter wetted by the fluid vein in m

Hence the speed :

$$V = \frac{20\ 000 \times 0.198.10^{-3}}{928.3 \times 20.10^{-3}} = 0.22\ m/s \qquad (123)$$

The velocity V is the same in all tubes. If q_v is the total volume flow rate, then the total cross-sectional area of the tubes is:

$$S = \frac{q_v}{V} = \frac{q_{mc}}{\rho}\frac{1}{V} = \frac{4.3}{928 \times 0.21} = 2.10^{-2} m^2 \qquad (124)$$

The number of tubes required to ensure the required flow rate is equal to:

$$N = \frac{S}{\pi d^2/4} = \frac{2.10^{-2}}{\pi \times (20.10^{-3})^2/4} = 63.6 \qquad (125)$$

As there must be an integer number of tubes, we'll take the next higher integer: $N = 64\ Tubes$

If the length of the bundle is L (which is also the length of each tube) the total exchange surface is: $\Sigma = N\pi dL$

We deduce:

$$L = \frac{\Sigma}{N\pi d} = \frac{8.27}{64 \times \pi \times 20.10^{-3}} = 2.05\ m \approx 2\ m \qquad (126)$$

4.8 Hypotheses on exchanger analysis

The previous analysis was based on the following hypotheses:

- ✓ The mass heat of the fluids remains substantially constant as they pass through the exchanger (practical = calculation of mass heats for average fluid conditions in the exchanger).

- ✓ The *k* coefficient remains essentially constant along the entire exchange surface which assumes that the fluid-wall convection coefficients are constant.

4.9 Intermediate circuit pump sizing

The aim of this paragraph is to size the circulator pump for the intermediate circuit between the two heat exchangers. The main data required to size a circulating pump are the flow rate to be conveyed and the head. The flow rate to be conveyed is already known as a function of the heating power to be circulated and the heating water speed.

Pressure drops and pressure supplied by the pump

To circulate a fluid, it is necessary to create a pressure difference with the fluid flowing from "high" to "low" pressures.

In a horizontal pipe water can only flow from point *A* to point *B* if the pressure at *A* is greater than that at *B*. This pressure difference (Δp) corresponds to the friction between the water and the pipe wall. It's called pressure drop. In a closed circuit it's the pump that generates the pressure difference enabling the water to circulate.

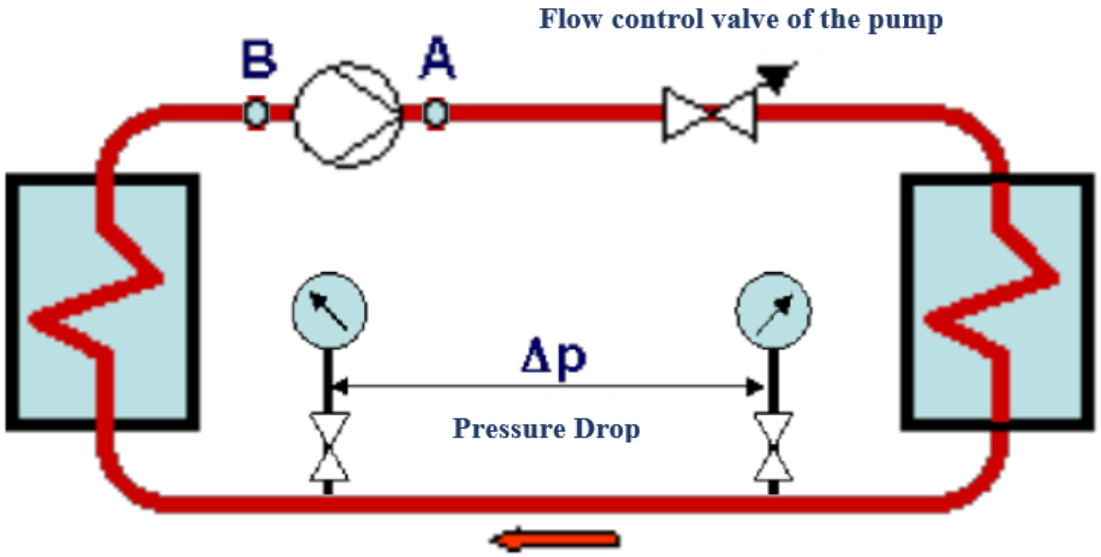

Figure 22. Intermediate hydraulic circuit. [16]

As shown in the figure 22, it is the pump that generates the pressure difference between *A* and *B*. This difference is called the pump's total head. Detailed calculations and parameters can be found in Appendix 12.

4.10 Motor sizing

4.10.1 Functionality

The gas engine is the heart of our cogenerator. Analytically, the operating cycle of a gas engine can be broken down like some internal combustion engines into four stages or phases, Piston movement is initiated by the combustion (rapid increase in temperature and therefore gas pressure) of a mixture of fuel and air (oxidizer) which takes place during the engine stroke. This is the only time when energy is produced. The other three strokes consume energy but make it possible. During start-up, the piston is moved by an external power source (often a starter motor: an electric motor is temporarily coupled to the crankshaft) until at least one stroke produces a force capable of sustaining the other three strokes before the next stroke. The motor then runs on its own producing torque on its output shaft.

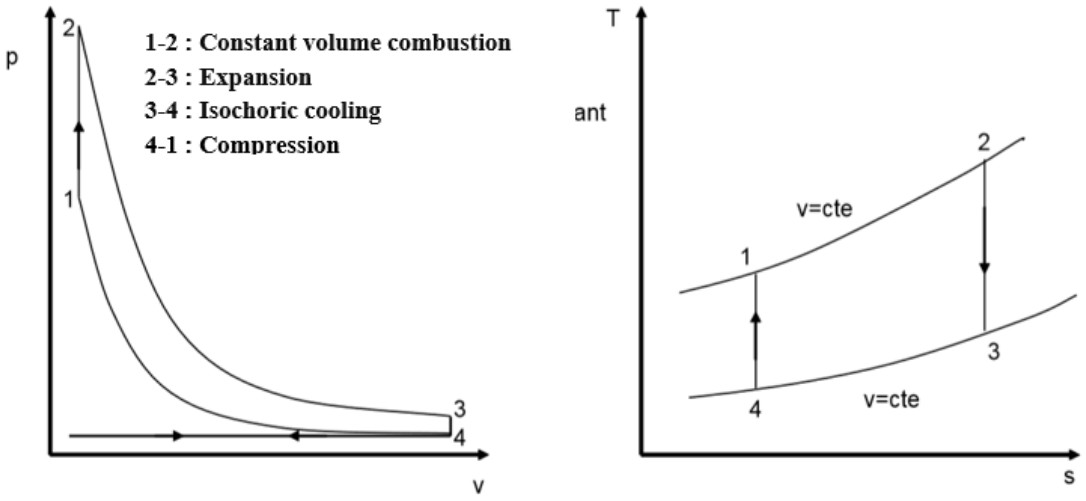

Figure 23. Beau de Rochas cycle. [17]

A description of the successive cycles of a four-stroke engine is shown in figure 23:

- Admission of a mixture of air and pulverized fuel. previously mixed and prepared by various components (carburetor or indirect injection system): opening of the intake valves and lowering of the piston which draws this mixture into the cylinder.
- Mixture compression: the intake valve closes then the piston rises compressing the mixture in the combustion chamber to 30 bars and 400 to 500 °C.
- Combustion and expansion near top dead center *(TDC):* the moment when the piston reaches its highest point and the compression is at its maximum. The spark plug, connected to a high-voltage ignition system, produces a spark a few degrees before

TDC. The initiated combustion that follows constitutes the power stroke. The hot gases at a pressure of 40 to 60 bars push the piston, initiating the movement.

- Exhaust: the exhaust valves open and the piston rises expelling the expanded burnt gases into the exhaust manifold.

The properties of the burnt gases estimated in the previous paragraph dictate the quantity of the air-gas mixture that will be drawn in by the cylinders. It is therefore necessary to return to the chemical equation of combustion and calculate the combustive power and smoke-producing power of the mixture (air-natural gas) in order to know the flow rate of each component.

4.10.2 Gas mixture composition

The table 10 presents the limiting characteristics of natural gas. Dry air is a homogeneous gas mixture. It is approximately composed in molar or volume fraction of 78.08% nitrogen, 20.95% oxygen and less than 1% other rare gases. In other words, "On average. 4.77 moles of air yield 1 mole of O_2 and 3.77 moles of N_2."

4.10.2.1 Calculation of combustibility

The quantity of air strictly necessary and sufficient to ensure neutral combustion of the natural gas fuel unit in gaseous state is calculated by this method:

$$V_{air} = \frac{V_{O_2}}{21\%} \quad (127) \quad With \quad V_{O_2} = \sum V_i$$

For a fuel with the general chemical formula:$C_x H_y O_z N_u S_v$ we define comburivor power with this expression

$$V_a = 4.77 \sum t_i \left[x_i + y_i + \frac{y_i}{4} - \frac{z_i}{2}\right] \qquad (128)$$

$$V_{a(CH_4)} = 4.77 \times 0.85\ [1 + 0 + 4/4 - 0/2] = 8.1090\ Nm^3/Nm^3 \qquad (129)$$

$$V_{a(C_2H_6)} = 4.77 \times 0.0885\ [2 + 0 + 6/4 - 0/2] = 1.4775\ Nm^3/Nm^3 \qquad (130)$$

$$V_{a(C_3H_8)} = 4.77 \times 0.0147\ [3 + 0 + 8/4 - 0/2] = 0.3506\ Nm^3/Nm^3 \qquad (131)$$

$$V_{a(C_4H_{10})} = 4.77 \times 0.0022\ [4 + 0 + 10/4 - 0/2] = 0.0682\ Nm^3/Nm^3 \qquad (132)$$

$$V_{a(C_5H_{12})} = 4.77 \times 0.0023\ [5 + 0 + 12/4 - 0/2] = 0.0877\ Nm^3/Nm^3 \qquad (133)$$

$$V_a = 10.09\ Nm^3/Nm^3$$

4.10.2.2 Smoke power calculation

The quantity of fumes resulting from the neutral combustion of the gaseous fuel unit is as follows:

$$V_f = \sum t_i[4.77(x_i + y_i) + 1.44y_i - 1.88z_i + 0.5u_i] \quad (134)$$

$$V_{f(CH_4)} = 0.85\ [4.77 + 1.44 \times 4] = 8.9505\ Nm^3/Nm^3 \quad (135)$$

$$V_{f(C_2H_6)} = 0.0885\ [4.77 \times 2 + 1.44 \times 6] = 1.6089\ Nm^3/Nm^3 \quad (136)$$

$$V_{f(C_3H_8)} = 0.00147\ [4.77 \times 3 + 1.44 \times 8] = 0.3797\ Nm^3/Nm^3 \quad (137)$$

$$V_{f(C_4H_{10})} = 0.0022\ [4.77 \times 4 + 1.44 \times 10] = 0.0736\ Nm^3/Nm^3 \quad (138)$$

$$V_{f(C_5H_{12})} = 0.0023\ [4.77 \times 5 + 1.44 \times 12] = 0.0946\ Nm^3/Nm^3 \quad (139)$$

$$V_{f(N_2)} = 0.029\ [4.77 \times 0 + 1.44 \times 0 + 1] = 0.029\ Nm^3/Nm^3 \quad (140)$$

$$V_{f(CO_2)} = 0.0114\ [4.77 + 0 - 1.88 \times 2] = 0.0115\ Nm^3/Nm^3 \quad (141)$$

$$V_{f(SO_2)} = 0.001\ [4.77 + 0 - 1.88 \times 2] = 0.00101\ Nm^3/Nm^3 \quad (142)$$

$$V_{f(H_2O)} = 0.0009\ [4.77 + 0 - 1.88 \times 2] = 0.0095\ Nm^3/Nm^3 \quad (143)$$

$$V_f = 11.15\ Nm^3/Nm^3$$

4.10.2.3 Calculation of excess combustion air

When combustion is not stoichiometric. it can be defined in several ways. generally, by its excess air *e*. or its deficiency of air *(- e).* or by the richness *R* or its inverse the air factor λ.

To examine how a non-stoichiometric reaction is written in terms of the air factor λ: In the case of excess air, λ is greater than 1 and there is too much oxygen. The reaction becomes:

$$CH_a + \lambda\left(1 + \frac{a}{4}\right)(O_2 + 3.76\ N_2) \rightarrow CO_2 + \frac{a}{2}H_2O + (\lambda - 1)\left(1 + \frac{a}{4}\right)O_2 + 3.76\ \lambda\left(1 + \frac{a}{4}\right)N_2 \quad (144)$$

λ is the multiplicative coefficient of the air term in this equation ($O_2 + 3.76N_2$).

$$R = \frac{1}{\lambda} \quad (145) \quad With \quad \lambda = 1 + e = \frac{1}{R} \quad (146)$$

With excess air e=60% such that $V_c' = V_c + \left(\frac{e}{100}\right)V_a$ (147)

This gives the following results:

Table 16. Combustible and smoke-producing with and without excess air

	Without excess air	With 60% excess air
Combustive power Nm^3/Nm^3	10.093	16.16
Smoke-producing power Nm^3/Nm^3	11.15	17.21

4.10.2.4 Calculating smoke density

The density of pure gaseous compounds is obtained by dividing their molar mass by that of air, which is equal to 28.9.

So, for carbon dioxide CO_2 whose molar mass is 44, its density is equal to:

$$d = \frac{M_{CO_2}}{M_{air}} = \frac{44}{28.9} = 1.52 \qquad (148)$$

Its density will be 1.52 times that of air.

$$\rho_{CO_2} = d \,.\, \rho_{air} \qquad (149)$$

The density of air depends on temperature and pressure under normal conditions, it is 1.2 kg/m^3.

The density of the fumes is therefore as follows:

$$M_{fumes} = \frac{M_t}{N_t} = \frac{462.69}{17.17} = 26.94\ g/mol \qquad (150)$$

$$d_{fumes} = \frac{M_{fumes}}{M_{air}} = \frac{26.94}{28.96} = 0.93 \qquad (151)$$

$$\rho_{fumes} = d_{fumes} \,.\, \rho_{air} = 1.188\ kg/m^3 \qquad (152)$$

4.10.3 Consumed gas flow

Back to the dry smoke power. or combustive power. from which we can determine the admissible fuel quantity. as well as the fresh air quantity. Given that we've already determined the flue gas flow rate (4.28 *kg/s*) entering the heat recovery exchanger (Table 17).

Table 17. Density and mass flow of gases

	Mass flow kg/s	Mass density kg/m^3
Air	4.05	1.200
Natural Gas	0.175	0.836
Fume	4.280	1.188

This generator consumes 514.8 kg of natural gas per hour. Taking into account that the combustion of one kilogram of gas requires 23.48 kg of air and produces 24.5 kg of fumes.

4.10.4 Combustion power

4.10.4.1 Calculation of the lower calorific value of combustion

The limiting characteristics of natural gas are as follows:

Table 18. Natural Gas LHV

Composition of NG	LHV (MJ/kg)	LHV (kJ/mol)	Molar mass (g/mol)	Molar fraction (%)	LHV partial (kJ/mol)
Methane	50.016	802.27	16.04	85	681.929
Ethane	47.794	1437.11	30.07	8.85	127.184
Propane	46.357	2044.13	44.1	1.47	30.048
Butane	45.752	2653.6	58.12	0.22	5.838
Pentane	45.357	3272.45	72.15	0.23	7.526
Sulfur	9.163	587.34	32.06	0.1	0.587
Natural gas	**46.892**	**853.112**	**18.193**		

With:

$$LHV_{Gas}(kJ/mol) = \sum LHV_i(kJ/mol) \times molar\ fraction \qquad (153)$$

$$LHV_{Gas}(MJ/kg) = LHV_{Gas}(kJ/mol)\ /\ molar\ mass \qquad (154)$$

$P_c = \dot{q}_{gas} LHV$ (155)

$With\ \ \dot{q}_{gas} = 1.75\ g/s$

So, the power produced by combustion is:

$$P_c = 270.10^{-3} \times 46.89 = 8.2\ MW \qquad (156)$$

Mechanical power

This motor is assumed to have a mechanical efficiency of 30%. We therefore deduce its useful power as follows: $P_{mec} = P_c\ .\eta = 8.2 \times 0.30 = 2.46\ MW$ (157)

4.11 Integrated Environmental and Financial Impact Assessment

4.11.1 Environmental impact assessment

Greenhouse gas emissions attributable to stationary combustion

This section describes the method and data required to estimate emissions attributable to our installation. as well as the category in which these emissions should be reported. Default

emission factors are used based on national energy statistics for all source categories and fuels (see Appendix 9).

In the sectoral approach. emissions attributable to stationary combustion are specified for a number of societal and economic activities defined in Sector 1A of the IPCC (Intergovernmental Panel on Climate Change) **[18]**.

Sector 1A (Fuel Combustion Activities) represents a detailed breakdown of the sector (electricity generation. oil refining. etc.) for stationary combustion. It involves emissions resulting from the intentional oxidation of materials in an apparatus designed to generate heat and provide it in the form of heat or mechanical work to a process. or intended for use outside the apparatus.

Emissions attributable to self-producers (public or private enterprises that produce electricity/heat entirely or partially for their own use. in support of their main activity) must be allocated to the sector where they were produced.

In general, emissions of each greenhouse gas attributable to stationary sources are calculated by multiplying the fuel consumption by the corresponding emission factor. For an estimate of CO_2 emissions. the following data is required for each source category and fuel:

- Data on the quantity of fuel burned in the source category
- A default emission factor

Emission factors come from default values provided with associated uncertainty ranges in the Appendix 9. The following equation is used: **[19]**

$$Emission_{GHG,GN} = Consumption\ Fuel_{GN} \times Emission_{GHG,GN} Factor$$

Annual production of the system Annual gas consumption savings case (Cogenerator): The installation consumes 0.175 kg/s of natural gas. i.e., to produce 4320 kWe. While the steam turbine consumes 1081 Kg /h = 0.3 kg/s to provide the same power because: Specific fuel consumption (SFC) = 2700 kCal/kWe

$$SFC = \frac{\dot{v}_{gas}.LHV}{P_e} \quad (158) \quad so \ \ \dot{v}_{gas} = \frac{P_e.SFC}{SFC} \qquad (159)$$

With:

SFC: Specific fuel consumption (average) in *kCal/kWh*.

$\dot{v}_{gas}$: Natural gas volumetric flow rate in (Nm3/h)

LHV: Higher Heating Value in *(kCal/Nm^3/h)*. It is the thermal energy released by the combustion of one kilogram of fuel. This energy includes the sensible heat and the latent heat of vaporization of water typically produced by combustion.

P_e : Electrical power produced in *(kWe)*.

Therefore, the gain in gas consumption is 0.3 – 0.175 = 0.125 kg/s.

Annual gain in gas consumption (with 60 days of unit shutdown) 3.294.000 kg/year.

4.11.2 Financial Statement

The monetary gains from the recovered amount of natural gas are calculated using the following formula:**[20]**

$$G_{GN} = E_s \times C_T \qquad (160)$$

With:

E_s : Annual energy savings in natural gas

C_T : Cost of one ton of oil equivalent (TOE) equal to 1200 DT/Toe

$$G_{NG} = 3294 * 1200 \qquad (161)$$

$$G_{NG} = \mathbf{3.952.800\ DT}$$

The approximate exchange rate in Euros is:

1 Tunisian dinar (TND) ≈ 0.29 euros (EUR)

Using this rate:

3.952.800 TND × 0.29 EUR/TND ≈ 1.146.312 EUR

So, 3.952.800 Tunisian dinars is approximately 1.146.312 euros.

5. Conclusions

This project focused on enhancing the energy efficiency at the CPR natural gas station by implementing a turbogenerator and optimizing the preheater system. The primary objective was to recover the expansion energy of natural gas and improve overall system performance. Key steps and findings include the assessment of the current system, the implementation of the turbogenerator, the optimization of the preheater system, significant energy savings and efficiency gains with financial and environmental impact analysis.

The specific steps taken were as follows:

Assessment of Current System:

- Evaluated the existing gas consumption patterns and identified inefficiencies in the thermal and mechanical systems.
- Determined the specific fuel consumption (SFC) and higher heating value (LHV) of natural gas, which were essential for calculating the energy savings.

Implementation of Turbogenerator:

- Installed a turbogenerator to capture the mechanical energy from the pressure drop of natural gas before it enters the boiler.
- This installation resulted in significant electrical energy generation, estimated to produce 4320 kWe.

Optimization of Preheater System:

- Added a preheater system designed to utilize superheated water at 180°C, with a flow rate of 5.3 kg/s, or alternatively, superheated steam from steam transformers.
- Calculated the desired thermal power of the preheater to be 2043 kW, ensuring the natural gas is preheated to 117°C for optimal combustion.

Energy Savings and Efficiency Gains:

- The cogeneration system's gas consumption was reduced by 0.125 kg/s, leading to an annual gas savings of approximately 3,294,000 kg.
- This reduction translated to an annual energy saving of 3,294 TOE (tons of oil equivalent).

Financial and Environmental Impact:

- The monetary gains from the recovered natural gas were calculated at 3,952,800 DT per year, equivalent to approximately 1,146,312 EUR.

- The project also contributed to a significant reduction in greenhouse gas emissions by decreasing the overall natural gas consumption.

Future Work:

- Further optimization of the system's efficiency and performance is recommended. This includes refining the design and operation of the preheater and turbogenerator.
- Evaluating the scalability of the technology for broader applications in other regions and exploring the integration of renewable energy sources to complement the recovered energy.
- Proposing policy changes to support the implementation of similar energy recovery systems across Tunisia.

In essence, the project successfully demonstrated the potential for significant energy recovery and efficiency improvements at the CPR natural gas station. By implementing a turbogenerator and optimizing the preheater system, the project not only enhanced energy generation but also reduced operational costs and environmental impact. These advancements mark a crucial step towards sustainable energy production and the efficient use of natural resources.

Reference

1. IEA Statistics © OECD/IEA (2014) . Electric power consumption (kWh per capita) - Tunisia.
2. Lakhoua, M.N. (2009). Mise à Niveau du Système de Comptage Gaz Naturel d'une Centrale Thermique. In 5th International Conference: Sciences of Electronic, Technologies of Information and Telecommunications, March 22-26, 2009, Tunisia.
3. Toshiba. (n.d.). Generation Technologies. Toshiba Global. Retrieved from https://www.global.toshiba/ww/products-solutions/thermal/products-technical-services/generation-technologies.html
4. La Société Tunisienne de l'Electricité et du Gaz (STEG)-Étude préparatoire du projet de construction de la centrale électrique à cycle combiné à Radès en Tunisie - Mars. 2014 Japan International Cooperation Agency (JICA) Tokyo Electric Power Services Co., LTD.
5. U.S. Department of Energy. (2008). Waste Heat Recovery: Technology and Opportunities in U.S. Industry. Prepared by BCS, Incorporated
6. Kondratiev, V. N. (2024). Combustion - Chemical Reactions, Heat, Oxidation. In Encyclopaedia Britannica. Fact-checked by The Editors of Encyclopaedia Britannica
7. Fonds de formation professionnelle de la construction. (2012). Manuel modulaire chauffage central-installations au gaz, volume 1 canalisations de gaz naturel. Bruxelles. FFPC.,
8. Moruzzi. L. (1989). Recover energy in natural gas by turboexpansion. Pipe line industry. Retrieved from: http://www.cryostar.com/web/greenenergy-system.php
9. Incropera. F.P., & DeWitt. D.P. (2002). Introduction to Heat Transfer. John Wiley & Sons. London.
10. Guilié. C. (2011). Cours de combustion 2ème partie Combustions réelles, combustibles complexes. Dunod, Paris.

11. Tunisian Company of Electricity and Gas. (2023). Pressure Regulating Station Diagram. Internal document received on November 13. 2023.

12. Efficiency Enhancement of Gas Turbine Systems with Air Injection Driven by Natural Gas Turboexpanders, MDPI.

13. The Engineering ToolBox (2003). Saturated Steam - Properties for Pressure in Bar.

14. Cryostar. (2006). Low-carbon technology for a cleaner world [Catalog]. Cryostat.

15. Chebouba. A. (1994). Etude paramétrique de la condensation dans un gazoduc. Magister Thesis. I.A.P. Boumerdes.

16. Bollinger. A.F. (1998). Système de récupération d'énergie pour la détente du gaz naturel, Gaz d'aujourd'hui, 3.

17. Produced by I. Aartun. NTNU 2002. Based on the program Allprops. Center for Applied Thermodynamic Studies. University of Idaho.

18. NF D 30-002 (novembre 1989). Chauffage - Gaz - Combustibles gazeux - Chaudières de chauffage central à eau chaude - Rendement conventionnel d'exploitation - Détermination des paramètres de performance.

19. Padet. J. (2014). Echangeurs Thermiques. Chapitre 4 : Détermination des coefficients d'échange dans les échangeurs à fluides séparés. Masson. Paris.

20. Messe. J.Y. (2014). Caractéristiques physiques de l'eau bouillante. Program: Thermovapor.

21. Bonin. B. (2006). Les pompes de chauffage (1er niveau). Document PDF

22. Mines ParisTech. (N.d.). Performance des moteurs alternatifs à combustion interne et principes de la suralimentation

23. Celik, F., Larson. E.D., & Williams. R.H. (2005). Transportation fuel from coal with low CO2 emissions. In M. Wilson. T. Morris. J. Gale. & K. Thambimuthu (Eds.). Proceedings of 7th International Conference on Greenhouse Gas Control Technologies. Elsevier Science, Oxford UK.

24. CCP (2005). Economic and cost analysis for CO_2 capture costs in the CO_2 capture project. Scenarios. In D.C. Thomas (Ed.). Capture and separation of carbon dioxide from combustion Sources. Volume 1 (pp. Page range). Elsevier Science, Oxford. UK.

25. Percell, P.B., & Ryan. M.J. (1987). Steady state optimization of gas pipeline network operation. In Proceedings of the 19th PSIG Annual Meeting. Tulsa. OK. October.

26. Benmansour. N. (2021). Chapitre II: Fluide caloporteur et échangeurs. In Cours: Conversion Photothermique. Fac. Des Sci. Dép. Physique M2. Energétique et Energies Renouvelables. University of M'Sila.

27. Association Amicale des Anciens Élèves de l'École de Thermique. (1982). Aide-mémoire du thermicien.

28. Moon. K. (2002). Analysis of LNG Tank Cooldown system. In Theories and Application of Chem. Eng., Vol. 8. No. 2.

29. Ansaldo Energia. Centrale Thermique de Rades Process and Instrumentation Diagram. Ansaldo Energia.

30. Tunisian Company of Electricity and Gas. (2023). Gas Heater. Internal document received on September 21. 2023.

31. Tunisian Company of Electricity and Gas. (2023). Steam Transformer Diagram. Internal document received on September 21. 2023.

32. Touloukian. Y.S., Powell. R.W., Ho. C.Y., & Klemens. P.G. (1970). Thermophysical properties of matter. Vol. 1: Thermal conductivity of metallic solids. IFI/Plenum Press.

33. Tunisian Company of Electricity and Gas. (2023). Analysis of Gas Consumed by Centrale Rades. Internal document received on September 21. 2023.

34. Gómez, D.R., Watterson. J.D., Americano. B.B.. Ha. C.. Marland. G., Matsika. E., Namayanga. L.N., Osman-Elasha. B., Saka. J.D.K., & Treanton. K. (2006). Guidelines for National Greenhouse Gas Inventories. Intergovernmental Panel on Climate Change (IPCC).

35. Perry. R.H., Green. D.W., & Maloney. J.O. (1997). Perry's Chemical Engineers' Handbook (7th ed.). McGraw-Hill.

36. Itieffe. (2022). Calcolo potenza elettropompe [Catalog]. Itieffe.

Appendices

Appendix 1. Fouling resistances [22]

Variation : 1.10^{-4} et 70.10^{-4} $(m^2.°C)/W$	
Eau de mer à T < 50°C	Re= 10^{-4} m²°C/W
Eau de mer à T > 50°C	Re= 2 10^{-4} m²°C/W
Eau de ville à T < 50°C	Re= 2 10^{-4} m²°C/W
Eau de ville à T > 50°C	Re= 3.5 10^{-4} m²°C/W
Eau de rivière	Re= 3.5 à 7 10^{-4} m²°C/W
Vapeur d'eau non grasse	Re= 10^{-4} m²°C/W
Vapeur d'eau grasse	Re= 2 10^{-4} m²°C/W
Liquides réfrigérants	Re= 1.8 10^{-4} m²°C/W
Fioul	Re= 4 à 9 10^{-4} m²°C/W
Essence, kérosène	Re= 2 10^{-4} m²°C/W
Huile de lubrification	Re= 1.8 10^{-4} m²°C/W
Air non dépoussiéré	Re= 3.5 10^{-4} m²°C/W
Produits de combustion gazeux	Re= 20 à 70 10^{-4} m²°C/W

Appendix 2. Solid-vapor equilibrium curve [23]

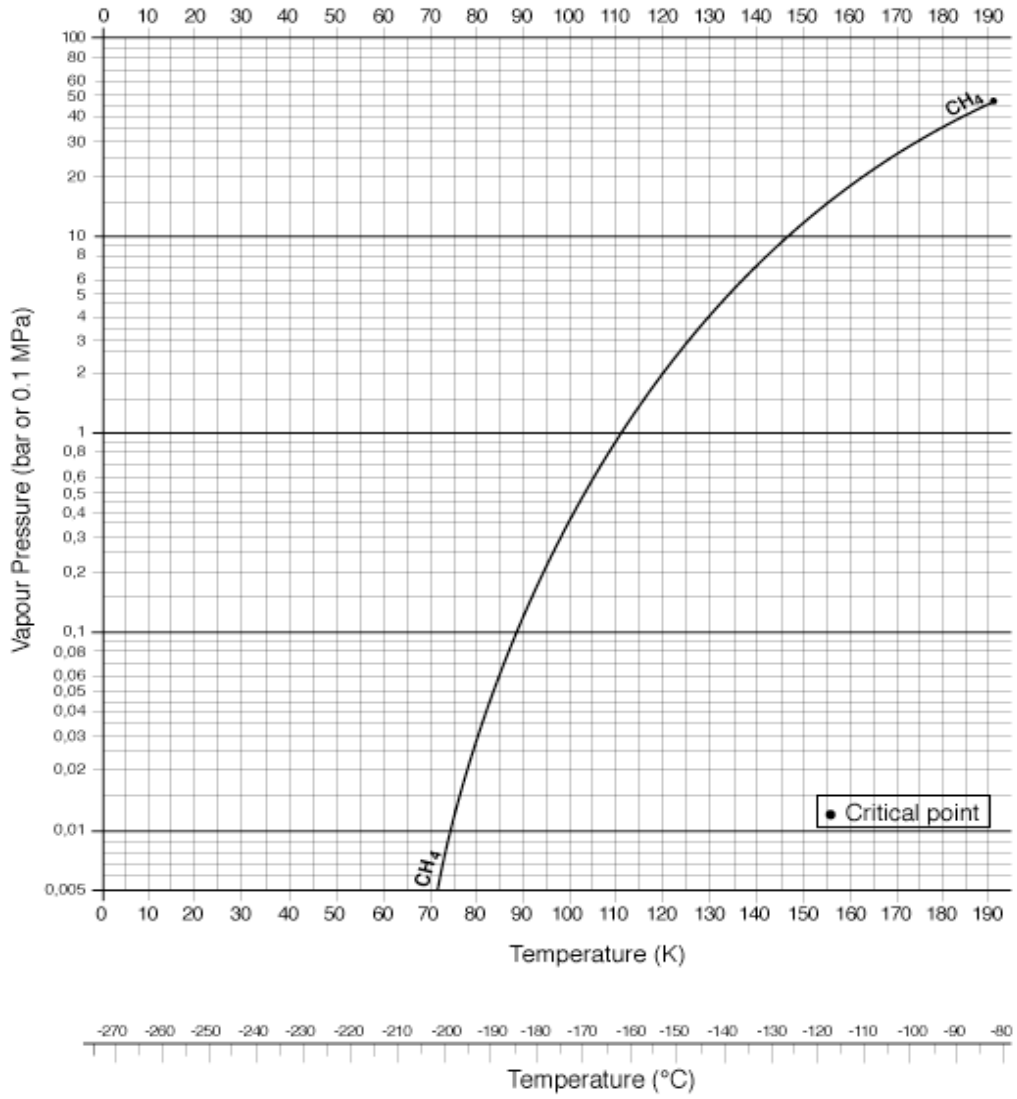

Appendix 3. PRS Stage-B [24]

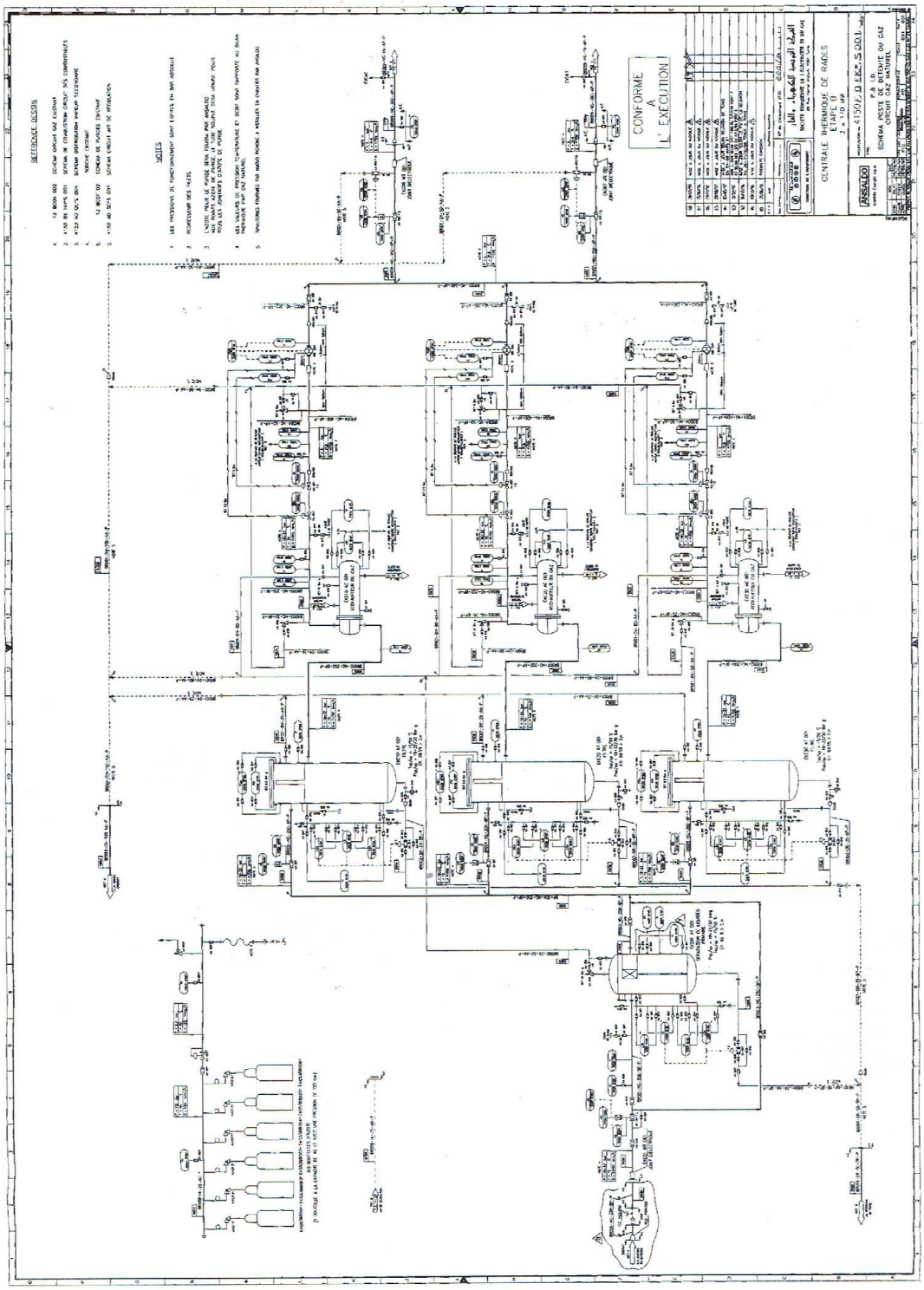

Appendix 4. Gas heater [25]

Manuel d'instructions du réchauffeur de gaz combustible

Réchauffeur de gaz combustible

Instructions opératoires

1. Détails de l'équipement

Type : Horizontal (avec réfrigérant de vidange)
A 4 tubes en "U" (débit de gaz à l'intérieur et débit de vapeur à l'extérieur)

Capacité : 59 300 Nm^3/h

Tempé. gaz : Entrée - 1°C
Sortie 7°C

Vapeur disponible : 6 bars abs. (5,1 kg/cm^2G), 158°C

(fluide)

Tempé. / vidange : 40°C

Consommation vapeur : 430 kg/h

Surface de chauffe : 46 m^2

Pression gaz : 20 bars abs (19,3 kg/cm^2G)

Pression de calcul : Côté tubes (gaz combustible)
25 bars abs. (24,5 kg/cm^2G)
Côté calandre (vapeur)
10,3 bars abs. (9,5 kg/cm^2G)

Température de calcul : Côté tubes (gaz combustible) 60°C
Côté calandre (vapeur) 185°C

Pression de l'épreuve hydrostatique
Côté tubes (gaz combustible)
37,5 bars abs. (37,2 kg/cm^2G)
Côté calandre (vapeur)
15,5 bars abs. (14,7 kg/cm^2G)

2. Construction

2-1 Nomenclature et matériaux

(1) Tôle de calandre(SM41B)

(2) Tôle de calandre(SM41B)

(3) Tôle de fond(SM41B)

(4) Tôle de fond(SM41B)

(5) Bride de calandre(SF45A)

(6) Bride de couvercle(SF45A)

(7) Plaque tubulaire(SF45A)

(8) Tube chauffant(ST335-SC)(?)

(9) Tirant(SS41)

(10) Entretoise(SGP)

(11) Chicane(SS41)

(12) Chicane longue(SS41)

(13) Plaque passe-cloison(SS41)

(14) Selle(SS41)

(15) Joint(V#520)

(16) Goujons & écrous(S43C/S350)

2-2 Détails du raccordement

2-3 Débit de gaz combustible

Comme l'indique le croquis de disposition de tubes, les tubes chauffants sont proprement disposés et divisés en quatre portions au moyen du faisceau tubulaire en "U" et des cloisons du couvercle. Il est donc prévu pour que le gaz combustible s'écoule dans les quatre chemins de tube.

a) Le gaz combustible s'écoule dans le couvercle(A) à travers la buse d'entrée du couvercle de calandre.

b) Le gaz combustible s'écoule dans les tubes chauffants dans la direction indiquée par les "flèches" du croquis.

c) Chauffé par de la vapeur, le gaz combustible sort de la buse de sortie prévue sur le couvercle de calandre(D).

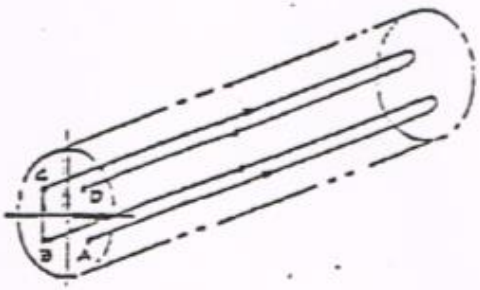

2-4 Débit de vapeur

a) La vapeur d'eau s'écoule dans la calandre à travers la buse d'entrée placée à la tête de la tôle fixée à la calandre.

b) Comme l'indique le croquis donné ci-dessous, l'échange de chaleur a lieu de telle sorte que la vapeur s'écoule à l'extérieur des tubes chauffants tout en réalisant le mouvement serpentin au moyen de la chicane ajustée à l'intérieur de la calandre.

(1) Entrée de vapeur & sortie de vidange

(2) Chicane longue

(3) Chicane

(4) Tube chauffant

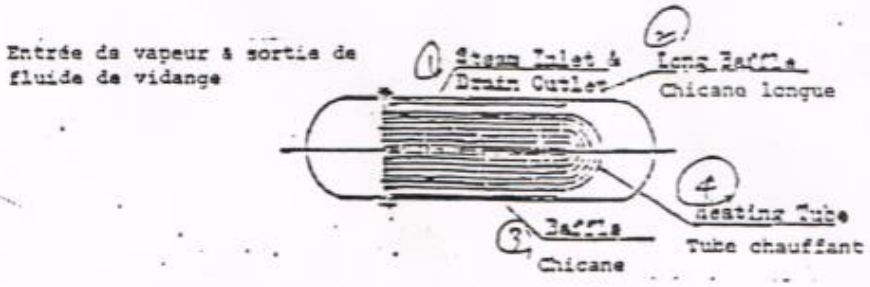

c) La vapeur d'eau devient du fluide de vidange pour sortir de la buse de sortie de vidange ajustée au fond de l'arrière de la calandre.

a) Le gaz combustible s'écoule dans le couvercle(A) à travers la buse d'entrée du couvercle de calandre.

b) Le gaz combustible s'écoule dans les tubes chauffants dans la direction indiquée par les "flèches" du croquis.

c) Chauffé par de la vapeur, le gaz combustible sort de la buse de sortie prévue sur le couvercle de calandre(D).

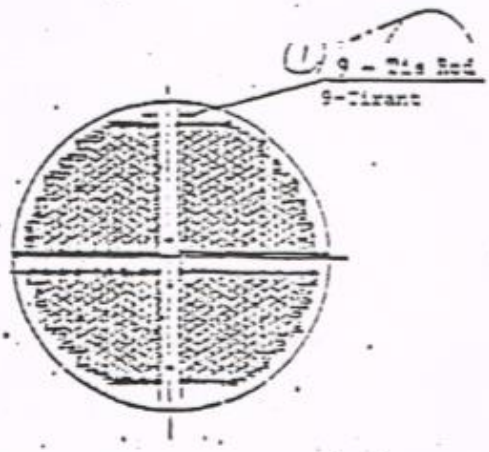

Instructions opératoires

1) Pour le présent réchauffeur, la partie supérieure du corps est chauffée par de la vapeur, et la partie inférieure, par le fluide de vidange de vapeur.
Dans ce cas, il faut réguler le niveau de fluide de vidange de telle sorte qu'il se trouve toujours au centre du corps.

2) Le niveau de fluide de vidange peut être régulé au moyen de la vanne de contrôle prévue à la buse de sortie de fluide de vidange. Normalement, les robinets d'entrée et de sortie de la vanne de contrôle de niveau de fluide de vidange sont en pleine ouverture, alors que le robinet de by-pass de cette vanne est fermé.
En cas de problème opératoire posé à cette vanne, les robinets d'entrée et de sortie en sont fermés, et le robinet de by-pass, manoeuvré en commande manuelle.

3) Contrôler parfois le niveau de fluide de vidange au moyen de l'indicateur de niveau.

4) La présence éventuelle d'air à l'intérieur du corps de réchauffeur (côté vapeur) est très nuisible au point de vue rendement thermique. Dans de tels cas, par conséquent, expulser de l'air à travers l'évent avant de procéder au fonctionnement du réchauffeur.

Appendix 5. Steam transformer [26]

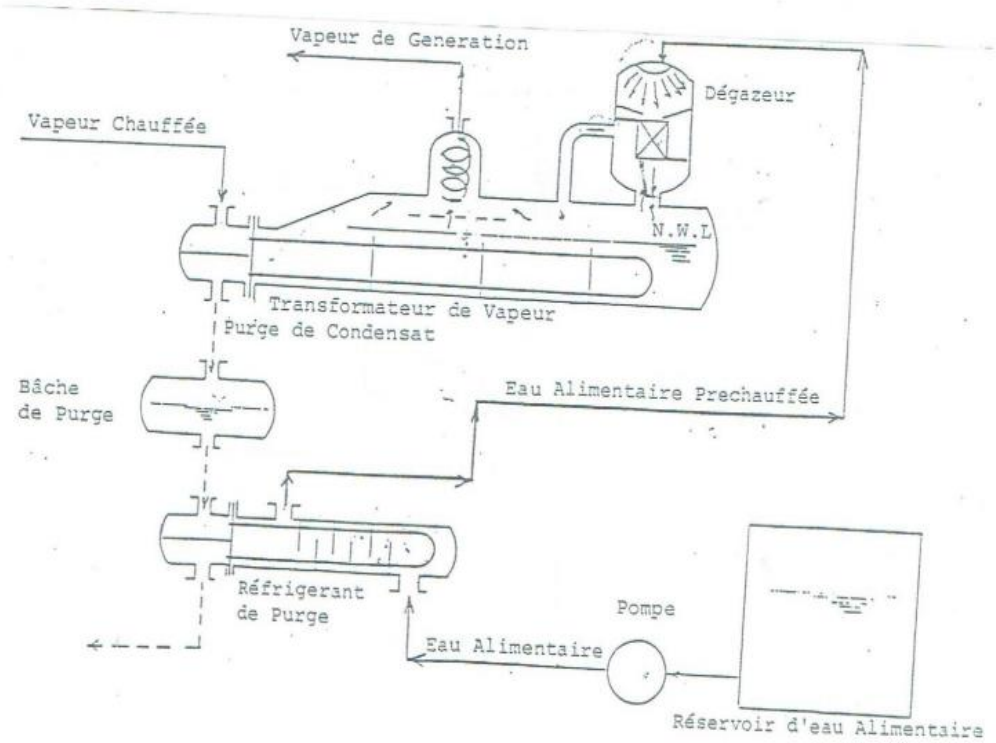

Appendix 6. Thermal conductivity of steel [27]

	c_p [J.kg^{-1}.K^{-1}]	ρ [kg.m^{-3}]	λ [W.m^{-1}K^{-1}]				
			T=100 K	T=200 K	T=300 K	T=400 K	T=600 K
Laiton	380	8530	75	95	110	137	149
Acier inoxydable (AISI 304 L)	468	8238			13,5	15,2	18,3

Tableau 1: *Propriétés thermiques connues du matériau utilisé [5]*

Appendix 7. Composition of natural gas [28]

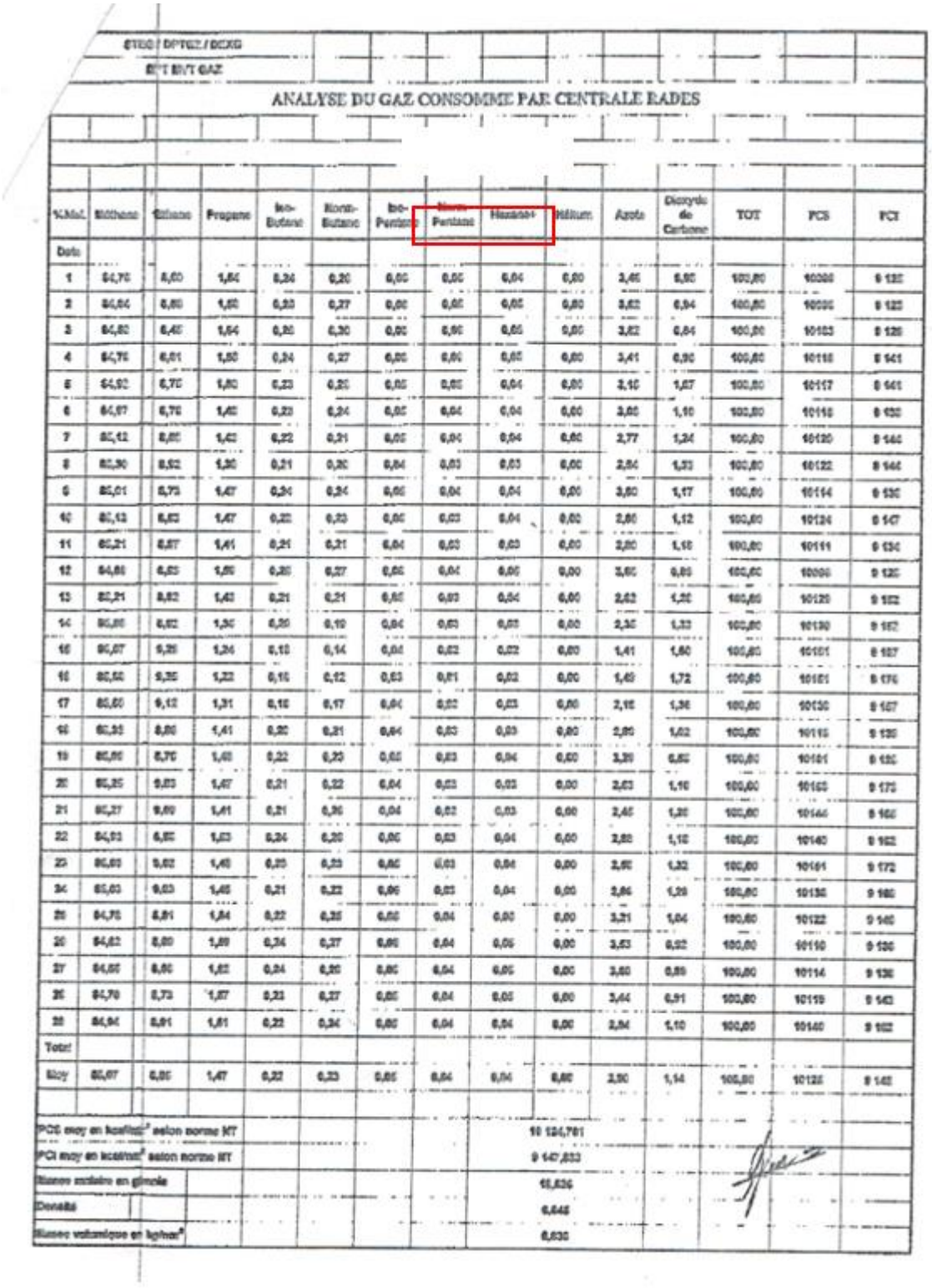

ETSO / DPTGZ / DCXG

EPT BVT GAZ

ANALYSE DU GAZ CONSOMME PAR CENTRALE RADES

%Mol	Méthane	Ethane	Propane	Iso-Butane	Normal-Butane	Iso-Pentane	Normal-Pentane	Hexanes+	Hélium	Azote	Dioxyde de Carbone	TOT	PCS	PCI
Date														
1	84,76	8,60	1,64	0,24	0,20	0,00	0,00	0,04	0,00	3,46	0,90	100,00	10088	9 135
2	84,84	8,60	1,60	0,23	0,27	0,00	0,00	0,05	0,00	3,62	0,94	100,00	10090	9 133
3	84,80	8,46	1,64	0,20	0,20	0,00	0,00	0,05	0,00	3,62	0,84	100,00	10103	9 126
4	84,76	8,61	1,60	0,24	0,27	0,00	0,00	0,05	0,00	3,41	0,90	100,00	10116	9 141
5	84,92	8,70	1,60	0,23	0,25	0,00	0,00	0,04	0,00	3,10	1,07	100,00	10117	9 141
6	84,87	8,76	1,60	0,23	0,24	0,00	0,04	0,04	0,00	3,00	1,10	100,00	10118	9 150
7	85,12	8,65	1,62	0,22	0,21	0,00	0,04	0,04	0,00	2,77	1,24	100,00	10120	9 140
8	85,30	8,52	1,50	0,21	0,20	0,04	0,03	0,03	0,00	2,84	1,33	100,00	10122	9 144
9	85,01	8,73	1,67	0,24	0,24	0,00	0,04	0,04	0,00	3,00	1,17	100,00	10114	9 136
10	85,13	8,62	1,67	0,22	0,23	0,00	0,03	0,04	0,00	2,80	1,12	100,00	10124	9 147
11	85,21	8,67	1,61	0,21	0,21	0,04	0,03	0,03	0,00	2,80	1,10	100,00	10111	9 134
12	84,86	8,63	1,66	0,20	0,27	0,00	0,04	0,00	0,00	3,00	0,93	100,00	10098	9 126
13	85,21	8,62	1,63	0,21	0,21	0,00	0,03	0,04	0,00	2,62	1,33	100,00	10120	9 132
14	85,05	8,62	1,50	0,20	0,19	0,04	0,03	0,03	0,00	2,30	1,33	100,00	10130	9 162
15	85,07	9,26	1,24	0,13	0,14	0,04	0,02	0,02	0,00	1,41	1,50	100,00	10101	9 167
16	85,50	9,35	1,22	0,15	0,12	0,03	0,01	0,02	0,00	1,40	1,72	100,00	10101	9 176
17	85,00	9,12	1,31	0,15	0,17	0,04	0,02	0,03	0,00	2,15	1,36	100,00	10130	9 167
18	85,35	8,80	1,41	0,20	0,21	0,04	0,03	0,03	0,00	2,00	1,02	100,00	10115	9 139
19	85,00	8,70	1,60	0,22	0,20	0,00	0,03	0,04	0,00	3,20	0,00	100,00	10101	9 135
20	85,25	8,63	1,47	0,21	0,22	0,04	0,03	0,03	0,00	2,63	1,10	100,00	10103	9 173
21	85,27	8,69	1,61	0,21	0,20	0,04	0,02	0,03	0,00	2,40	1,20	100,00	10144	9 160
22	84,91	8,82	1,63	0,24	0,20	0,00	0,03	0,04	0,00	2,80	1,10	100,00	10140	9 162
23	85,03	8,62	1,48	0,20	0,23	0,00	0,03	0,04	0,00	2,90	1,32	100,00	10161	9 172
24	85,03	8,63	1,45	0,21	0,22	0,00	0,03	0,04	0,00	2,86	1,20	100,00	10130	9 160
25	84,76	8,81	1,64	0,22	0,25	0,00	0,04	0,00	0,00	3,21	1,04	100,00	10122	9 140
26	84,82	8,80	1,69	0,24	0,27	0,00	0,04	0,05	0,00	3,03	0,02	100,00	10110	9 130
27	84,85	8,80	1,62	0,24	0,20	0,00	0,04	0,05	0,00	3,00	0,89	100,00	10114	9 136
28	84,76	8,73	1,67	0,23	0,27	0,00	0,04	0,05	0,00	3,04	0,91	100,00	10119	9 143
29	84,84	8,81	1,61	0,22	0,24	0,00	0,04	0,04	0,00	2,84	1,10	100,00	10140	9 162
Total														
Moy	85,07	8,65	1,47	0,22	0,23	0,00	0,04	0,04	0,00	2,90	1,14	100,00	10125	9 145

PCS moy en kcal/m³ selon norme MT	10 124,781
PCI moy en kcal/m³ selon norme MT	9 147,833
Masse molaire en g/mole	16,836
Densité	0,648
Masse volumique en kg/m³	0,838

Appendix 8. Cross-flow [14] One fluid mixed at Qt min an un-mixed fluid: fluid controlling the transfer (Cmin) un-mixed

Type de circulation	$E\ (NUT, R)$	$NUT\ (E, R)$	Cas particulier	E_{lim} pour $NUT = +\infty$
Contre-courant	$E = \frac{1 - \exp.[-(1-R)NUT]}{1 - R\exp.[-(1-R)NUT]}$	$NUT = \frac{1}{1-R}\ell n\left(\frac{1-ER}{1-E}\right)$	$R=0$ $E = 1-\exp.(-NUT)$ $NUT = \ell n[1/(1-E)]$ $R=1$ $E = NUT/(1+NUT)$ $NUT = E/(1-E)$	$E_{lim} = 1$ *qq* soit R
Courants croisés fluide non brassé	$E = \frac{1}{R\,NUT}\sum_{n=0}^{n=\infty} F_n(NUT)\,F_n(R\,NUT)$ $F_n(x) = 1-\exp.^{-x}\sum_{p=0}^{p=n}\frac{x^p}{p!}$		$R=0$ $E = 1-\exp.(-NUT)$	$E_{lim} = 1$ *qq* soit R
Courants croisés 1 fluide brassé à q_t^{min}	$E = \frac{1}{R}(1-\exp.[-R.\Gamma])$ avec $\Gamma = 1-\exp.[-NUT]$	$NUT = -\ell n\left[1+\frac{1}{R}\ell n(1-ER)\right]$	$R=0$ $E = 1-\exp.(-NUT)$	$E_{lim} = \frac{1}{R}(1-\exp.(-R))$
(1-N)	$E = \frac{2}{(1+R)+\sqrt{1+R^2}\,\frac{1+\exp.[-NUT\sqrt{1+R^2}]}{1-\exp.[-NUT\sqrt{1+R^2}]}}$	$NUT = \frac{1}{\sqrt{1+R^2}}\ell n\,\frac{2-E(1+R-\sqrt{1+R^2})}{2-E(1+R+\sqrt{1+R^2})}$	$R=0$ $E = 1-\exp.(-NUT)$	$E_{lim} = \frac{2}{1+R+\sqrt{1+R^2}}$
Co-courant	$E = \frac{1}{1+R}[1-\exp.[-(1+R)NUT]]$	$NUT = -\frac{1}{1+R}\ell n\,[1+E(1+R)]$	$R=0$ $E = 1-\exp.(-NUT)$	$E_{lim} = \frac{1}{1+R}$

Appendix 9. CO_2 emission factor of natural gas [29]

TABLEAU 2.2 (SUITE)
FACTEURS D'EMISSION PAR DEFAUT POUR LA COMBUSTION STATIONNAIRE DANS LES INDUSTRIES ENERGETIQUES
(kg de gaz à effet de serre par TJ sur une base calorifique nette)

Combustible		CO_2			CH_4			N_2O		
		Facteur d'émission par défaut	Limite inférieure	Limite supérieure	Facteur d'émission par défaut	Limite inférieure	Limite supérieure	Facteur d'émission par défaut	Limite inférieure	Limite supérieure
Goudron de houille		n 80 700	68 200	95 300	n 1	0,3	3	r 1,5	0,5	5
Gaz dérivés	Gaz d'usine à gaz	n 44 400	37 300	54 100	n 1	0,3	3	0,1	0,03	0,3
	Gaz de four à coke	n 44 400	37 300	54 100	r 1	0,3	3	0,1	0,03	0,3
	Gaz de hauts fourneaux	n 260 000	219 000	308 000	r 1	0,3	3	0,1	0,03	0,3
	Gaz de convertisseur à l'oxygène	n 182 000	145 000	202 000	r 1	0,3	3	0,1	0,03	0,3
Gaz naturel		56 100	54 300	58 300	r 1	0,3	3	0,1	0,03	0,3
Déchets municipaux (fraction non biomasse)		n 91 700	73 300	121 000	30	10	100	4	1,5	15
Déchets industriels		n 143 000	110 000	183 000	30	10	100	4	1,5	15
Huiles résiduelles		n 73 300	72 200	74 400	30	10	100	4	1,5	15
Tourbe		106 000	100 000	108 000	n 1	0,3	3	n 1,5	0,5	5

Appendix 10. The specific heat capacities (*Cp)* of various compounds at different temperature [21]

Compound	100 °C	500 °C	1000 °C	1500°C	2000 °C
N_2	1.042	1.115	1.215	1.268	1.297
O_2	0.933	1.048	1.122	1.163	1.200
CO_2	0.913	1.154	1.290	1.349	1.357
CO	1.044	1.132	1.230	1.279	1.306
H_2O	1.890	2.131	2.482	2.755	2.938
Air	1.010	1.092	1.184	1.234	1.265

Appendix 11. Properties of water [30]

T °C	ρ kg/m^3	μ $kg/m.s$	ν m^2/s	c_p $J/kg.K$	λ $W/m.K$	a m^2/s	Pr	β $1/Kelvin$
		EAU						
0	1002	$1,78.10^{-3}$	$0,179.10^{-5}$	4218	0,552	$13,1.10^{-8}$	13,6	$0,66.10^{-4}$
10	1001	$1,30.10^{-3}$	$0,130.10^{-5}$	4192	0,586	$13,7.10^{-8}$	9,30	$0,88.10^{-4}$
20	1001	$1,00.10^{-3}$	$0,101.10^{-5}$	4182	0,597	$14,3.10^{-8}$	7,02	$2,06.10^{-4}$
40	994,6	$0,651.10^{-3}$	$0,0658.10^{-5}$	4178	0,628	$15,1.10^{-8}$	4,34	$3,72.10^{-4}$
60	985,4	$0,469.10^{-3}$	$0,0477.10^{-5}$	4184	0,651	$15,5.10^{-8}$	3,02	$5,15.10^{-4}$
80	974,1	$0,354.10^{-3}$	$0,0364.10^{-5}$	4196	0,668	$16,4.10^{-8}$	2,22	$6,55.10^{-4}$
100	960,6	$0,281.10^{-3}$	$0,0294.10^{-5}$	4216	0,680	$16,8.10^{-8}$	1,74	$7,49.10^{-4}$
120	945,3	$0,234.10^{-3}$	$0,0247.10^{-5}$	4250	0,685	$17,1.10^{-8}$	1,446	$8,92.10^{-4}$
140	928,3	$0,198.10^{-3}$	$0,0214.10^{-5}$	4283	0,684	$17,2.10^{-8}$	1,241	$10,0.10^{-4}$
160	909,7	$0,172.10^{-3}$	$0,0189.10^{-5}$	4342	0,680	$17,3.10^{-8}$	1,099	$10,7.10^{-4}$
180	889,0	$0,154.10^{-3}$	$0,0173.10^{-5}$	4417	0,675	$17,2.10^{-8}$	1,004	$11,4.10^{-4}$
200	866,7	$0,138.10^{-3}$	$0,0160.10^{-5}$	4505	0,665	$17,1.10^{-8}$	0,937	$14,1.10^{-4}$
220	842,4	$0,125.10^{-3}$	$0,0149.10^{-5}$	4610	0,653	$16,8.10^{-8}$	0,891	$15,0.10^{-4}$
240	815,7	$0,117.10^{-3}$	$0,0143.10^{-5}$	4756	0,635	$16,4.10^{-8}$	0,871	$18,0.10^{-4}$
260	785,9	$0,108.10^{-3}$	$0,0137.10^{-5}$	4949	0,611	$15,6.10^{-8}$	0,874	$21,3.10^{-4}$
280	752,5	$0,102.10^{-3}$	$0,0135.10^{-5}$	5208	0,580	$14,8.10^{-8}$	0,910	$26,8.10^{-4}$
300	714,3	$0,096.10^{-3}$	$0,0135.10^{-5}$	5728	0,540	$13,2.10^{-8}$	1,019	

Appendix 12. Pump calculations [31]

itieffe.com 13/10/2022

Calcolo potenza elettropompe			B6.4
Se quello che stai usando ti è utile, premia il nostro lavoro - Guarda come ▶			
Calcolo della potenza necessaria al motore elettrico			
Selezionando il tipo di elettropompa, si ottengono risultati sufficientemente attendibili, utili per la valutazione della potenza necessaria			
Dati di calcolo			
Tipo di elettropompa ▶	centrifuga generica 1.450 giri/min		
	misura	Simbolo	valore
Temperatura acqua (0÷100°C - 32÷212°F) ▶	gradi centigradi	°C	90,0
Potata acqua ▶	metro cubo ora	Q	15,5
Prevalenza della pompa ▶	m H2O	H	80,0
Rendimento totale della pompa ▶	Adimensionale	μ	0,75
Riferimenti			

Rendimento della pompa	min	max
per pompe piccole ▶	0,4	0,6
per pompe medie ▶	0,6	0,75
per pompe grandi ▶	0,75	0,85

Risultato		
Assorbimento all'asse ▶	kW	5,65
Aumento percentuale (15 - 25%) ▶	%	25
Assorbimento totale motore ▶	kW	7,06